

Electronic Thesis and Dissertation Repository

---

12-10-2012 12:00 AM

## Fractional Condensation of Bio-Oil Vapors

Akhil Tumbalam Gooty, *The University of Western Ontario*

Supervisor: Franco Berruti, *The University of Western Ontario*

A thesis submitted in partial fulfillment of the requirements for the Master of Engineering Science degree in Chemical and Biochemical Engineering

© Akhil Tumbalam Gooty 2012

Follow this and additional works at: <https://ir.lib.uwo.ca/etd>

 Part of the [Other Chemical Engineering Commons](#)

---

### Recommended Citation

Tumbalam Gooty, Akhil, "Fractional Condensation of Bio-Oil Vapors" (2012). *Electronic Thesis and Dissertation Repository*. 979.

<https://ir.lib.uwo.ca/etd/979>

This Dissertation/Thesis is brought to you for free and open access by Scholarship@Western. It has been accepted for inclusion in Electronic Thesis and Dissertation Repository by an authorized administrator of Scholarship@Western. For more information, please contact [wlsadmin@uwo.ca](mailto:wlsadmin@uwo.ca).

# FRACTIONAL CONDENSATION OF BIO-OIL VAPORS

(Thesis format: Integrated Article)

by

Akhil Tumbalam Gooty

Graduate Program in Engineering Science  
Department of Chemical and Biochemical Engineering

A thesis submitted in partial fulfillment  
of the requirements for the degree of  
Master of Engineering Science (MEngSc)

The School of Graduate and Postdoctoral Studies  
The University of Western Ontario  
London, Ontario, Canada

© Akhil Tumbalam Gooty 2013

THE UNIVERSITY OF WESTERN ONTARIO  
School of Graduate and Postdoctoral Studies

**CERTIFICATE OF EXAMINATION**

Joint-Supervisor

Examiners

\_\_\_\_\_  
Dr. Franco Berruti

\_\_\_\_\_  
Dr. Charles Xu

Joint-Supervisor

\_\_\_\_\_  
Dr. Lars Rehmann

\_\_\_\_\_  
Dr. Cedric Briens

\_\_\_\_\_  
Dr. Jason Gerhard

The thesis by

**Akhil Tumbalam Gooty**

entitled:

**Fractional Condensation of Bio-oil Vapors**

is accepted in partial fulfillment of the  
requirements for the degree of  
Masters of Engineering Science

\_\_\_\_\_  
Date

\_\_\_\_\_  
Chair of the Thesis Examination Board

## **Abstract**

The research project described in this thesis deals with an investigation on the fractional condensation of bio-oil vapors to improve the separation of some of the key components of the bio-oil and, consequently, improve the properties and the value of each of the separated product streams.

In the first part, the separation of a mixture of three model compounds of bio-oil from a vapor and carrier gas stream was investigated with the help of a series of three condensers maintained at different temperatures. The practical performance of the fractional condensation train was improved by comparing the experimental results with the theoretical results predicted by the HYSYS modeling tool. It showed that good heat transfer and mixing was essential, and could be achieved by using condensers with a cyclonic entry. It also showed that a good demister was essential to achieve effective separation.

The second and third parts of the investigation focused on the fractional condensation of actual bio-oil vapors produced from the pyrolysis of two different biomasses: birch bark and Kraft lignin, respectively. In both cases, the temperatures of the condensers were optimized in order to separate the water present in the bio-oil vapor stream and increase the quality and the stability of the remaining bio-oil. The condenser train consisted of a condenser-cum-electrostatic precipitator (C-ESP) installed between two cyclonic condensers. The water content of the fractionated bio-oil was found to be less than 1 wt% with both biomasses. In case of Kraft lignin, the phenolics recovered in different bio-oil fractions were also analyzed. The effect of pyrolysis temperature on the fractionated bio-oil yield and characteristics was investigated.

Keywords: Pyrolysis, Bio-oil, Fractional condensation, Birch bark, Lignin, HYSYS,  
Electrostatic precipitator, phenols

## Co-Authorship Statement

### Chapter 2

<b>Article Title:</b> Fractional condensation of model compounds of bio-oil
<b>Authors:</b> Akhil Tumbalam Gooty, Cedric Briens, Franco Berruti
<b>Article Status:</b> Yet to be submitted for publication
<b>Contributions:</b> Akhil Tumbalam Gooty performed all experimental work, data analysis, process development and writing. Cedric Briens and Franco Berruti provided guidance, supervision and revised drafts of the work.

### Chapter 3

<b>Article Title:</b> Fractional condensation of bio-oil vapors produced from birch bark pyrolysis
<b>Authors:</b> Akhil Tumbalam Gooty, Dongbing Li, Cedric Briens, Franco Berruti
<b>Article Status:</b> Yet to be submitted for publication
<b>Contributions:</b> Akhil Tumbalam Gooty and Dongbing Li performed all experimental work and process development. Akhil Tumbalam Gooty completed data analysis and writing. Cedric Briens and Franco Berruti provided guidance, supervision and revised drafts of the work.

### Chapter 4

<b>Article Title:</b> Lignin pyrolysis and fractional condensation of its bio-oil vapors
<b>Authors:</b> Akhil Tumbalam Gooty, Dongbing Li, Franco Berruti, Cedric Briens
<b>Article Status:</b> Yet to be submitted for publication
<b>Contributions:</b> Akhil Tumbalam Gooty and Dongbing Li performed all experimental work and process development. Akhil Tumbalam Gooty completed data analysis and writing. Cedric Briens and Franco Berruti provided guidance, supervision and revised drafts of the work.

## **Dedication**

This thesis is dedicated to my beloved parents.

## **Acknowledgments**

First and foremost, I would like to express my deepest gratitude to my supervisors, Dr. Cedric Briens and Dr. Franco Berruti, for their continuous guidance and encouragement during my master's program.

I am very thankful to Dr. Dongbing Li, who has provided greatest support while working on the fractionation of bio-oil vapors. I would like to thank Rob Taylor for the timely assistance in procurement and installation of equipment required for the setup of fractional condensation train. I am also thankful to Caitlin Marshall for her help during the analysis of bio-oil samples. I would like to thank Javeed Mohammad for his help and advice during my initial days at Institute for Chemicals and Fuels from Alternative Resources (ICFAR).

I am thankful to each and every one who had encouraged me and helped me during the course of last two years.

## Table of Contents

CERTIFICATE OF EXAMINATION .....	ii
Abstract .....	iii
Co-Authorship Statement.....	v
Dedication .....	vi
Acknowledgments.....	vii
Table of Contents .....	viii
List of Tables .....	xi
List of Figures .....	xii
1 Chapter 1: Introduction .....	1
1.1 Fast pyrolysis .....	1
1.2 Bio-oil .....	3
1.2.1 Heating value .....	4
1.2.2 Water content .....	5
1.2.3 Acidity and Corrosiveness .....	5
1.2.4 Oxygen content .....	5
1.2.5 Stability .....	6
1.3 Fractionation of bio-oils.....	6
1.4 Aspen HYSYS .....	8
1.5 Research Objectives.....	9
1.6 References.....	10
2 Chapter 2: Fractional condensation of model compounds of bio-oil.....	12
2.1 Introduction.....	12
2.2 Materials and methods .....	15

2.2.1	Continuous Feeding System .....	15
2.2.2	Condensing System.....	16
2.2.3	Determination of the condensate composition.....	18
2.3	Experimental results and discussion .....	18
2.3.1	HYSYS simulation to select condenser temperatures .....	19
2.3.2	Heat transfer in condensers .....	20
2.3.3	Mixing and condensate composition .....	23
2.3.4	Yield of Condensers.....	26
2.4	Conclusions.....	36
2.5	References.....	37
3.	Chapter 3: Fractional condensation of bio-oil vapors produced from birch bark pyrolysis .....	39
3.1	Introduction.....	39
3.2	Materials and methods .....	41
3.2.1	Materials .....	41
3.2.2	Bubbling fluidized bed setup .....	41
3.2.3	Condensing system .....	43
3.2.4	Bio-oil production.....	46
3.2.5	Analysis of bio-oil fractions.....	47
3.3	Experimental results and discussion .....	47
3.3.1	Optimization of the fractional condensation train .....	48
3.3.2	Comparison with other fractional condensation trains .....	54
3.3.3	Optimization of pyrolysis reaction temperature .....	56
3.3.4	Fractioned birch bark bio-oil as a bio-fuel, comparison with traditional fuels.....	60
3.4	Conclusions.....	61
3.5	Acknowledgments.....	62

3.6	References.....	62
4	Chapter 4: Lignin pyrolysis and fractional condensation of its bio-oil vapors .....	64
4.1	Introduction.....	64
4.2	Materials and methods .....	66
4.2.1	Materials .....	66
4.2.2	Bubbling fluidized bed setup .....	67
4.2.3	Condensing system .....	69
4.2.4	Bio-oil production.....	72
4.2.5	Analysis of bio-oil fractions.....	73
4.3	Experimental results and discussion .....	74
4.3.1	Optimization of fractional condensation train .....	75
4.3.2	Optimization of operating conditions of pyrolysis .....	82
4.3.3	Fractioned lignin bio-oil as a biofuel .....	86
4.4	Conclusions.....	87
4.5	Acknowledgments.....	88
4.6	References.....	88
5	Chapter 5: Conclusions .....	90
5.1	Recommendations for future work .....	91
	Curriculum Vitae .....	92

## List of Tables

<b>Table 1.1</b> Typical properties of wood pyrolysis bio-oil and heavy fuel oil .....	4
<b>Table 2.1</b> Operating conditions used in all the experiments carried out using liquid mixture consisting of three model compounds (Glycerol: Ethylene glycol: Water = 0.33 wt%: 0.33 wt%: 0.33 wt%) .....	22
<b>Table 2.2</b> Operating conditions used in all the experiments carried out using liquid mixture consisting of two model compounds (Ethylene glycol: Water = 0.66 wt%: 0.34 wt%).....	23
<b>Table 2.3</b> Comparison of mass of liquid collected in condenser 1 with HYSYS predictions for different experimental conditions.....	27
<b>Table 2.4</b> Performance indices in presence of different mist collectors for the three-component model mixture .....	35
<b>Table 3.1</b> Operating conditions used in all the experiments performed for the fractional condensation of bio-oil vapors produced from birch bark pyrolysis .....	48
<b>Table 3.2</b> Comparison of physical properties of the bio-oil fractions obtained from two fractional condensation systems .....	55
<b>Table 3.3</b> Differences in design and operating parameters of the two fractional condensation systems .....	56
<b>Table 4.1</b> Details of GC-MS/FID system.....	74
<b>Table 4.2</b> Operating conditions used in all the experiments performed for the fractional condensation of bio-oil vapors produced from lignin pyrolysis .....	75

## List of Figures

<b>Figure 1.1</b> Conceptual process flow diagram of fast pyrolysis process.....	3
<b>Figure 2.1</b> Process Flow Diagram of model compounds feeding system and condenser train .....	16
<b>Figure 2.2</b> Glycerol % Recovery and % Purity as functions of Temperature of Condenser 1, as predicted with HYSIS.....	20
<b>Figure 2.3</b> Ethylene glycol % Recovery and % Purity as functions of Temperature of Condenser 2, as predicted with HYSIS.....	20
<b>Figure 2.4</b> Temperature Profile along the Condenser Train .....	21
<b>Figure 2.5</b> Composition of condensate in Condenser 1 at different nitrogen flow rates .....	25
<b>Figure 2.6</b> Composition of condensate in Condenser 1 at different condenser temperatures	26
<b>Figure 2.7</b> Comparison of experimental yields of three condensers to HYSYS results .....	28
<b>Figure 2.8</b> Effect of nitrogen flow rate on mist collection in first condenser .....	29
<b>Figure 2.9</b> Effect of temperature on mist collection in first condenser.....	30
<b>Figure 2.10</b> Effect of aluminum fan blade on mist collection in first condenser.....	31
<b>Figure 2.11</b> Effect of internals on mist collection in first condenser .....	33
<b>Figure 2.12</b> Comparison of the yields of individual components predicted by HYSYS to the yields achieved with stainless steel wool demister in the first condenser .....	36
<b>Figure 3.1</b> Schematic of bubbling fluidized bed setup used for the pyrolysis of birch bark .	43
<b>Figure 3.2</b> Schematic of fractional condensing train used for the collection of birch bark bio- oil .....	46
<b>Figure 3.3</b> Bio-oil yield in three condensers at different C-ESP temperatures.....	50
<b>Figure 3.4</b> Yields of oil fraction, water fraction, and raw bio-oil at different C-ESP temperatures .....	51
<b>Figure 3.5</b> Water content of oil fraction, water fraction, and raw bio-oil at different C-ESP temperatures .....	52
<b>Figure 3.6</b> Heating value of raw bio-oil, oil and water fractions at different C-ESP temperatures .....	53
<b>Figure 3.7</b> Energy recovered in the oil and water fractions at different C-ESP temperatures	54

<b>Figure 3.8</b> Yields of raw bio-oil, oil and water fractions at different pyrolysis temperatures	57
<b>Figure 3.9</b> Water content of raw bio-oil, oil and water fractions at different pyrolysis temperatures .....	58
<b>Figure 3.10</b> Heating value of raw bio-oil, oil and water fractions at different pyrolysis temperatures .....	59
<b>Figure 3.11</b> Energy recovered in oil fraction at different pyrolysis temperatures .....	60
<b>Figure 3.12</b> Heating value of dry bio-oil and other commercial fuels .....	61
<b>Figure 4.1</b> Schematic of bubbling fluidized bed setup used for the pyrolysis of lignin .....	68
<b>Figure 4.2</b> Mechanical stirrer used in the fluidized bed .....	69
<b>Figure 4.3</b> Agglomeration in the fluidized bed in the absence of mechanical stirrer .....	69
<b>Figure 4.4</b> Schematic of fractional condensing train used for the collection of lignin bio-oil .....	72
<b>Figure 4.5</b> Bio-oil yield in three condensers for different C-ESP temperatures .....	76
<b>Figure 4.6</b> Yields of oil fraction, water fraction, and raw bio-oil at different C-ESP temperatures .....	78
<b>Figure 4.7</b> Water content of oil fraction, water fraction, and raw bio-oil at different C-ESP temperatures .....	78
<b>Figure 4.8</b> Heating value of raw bio-oil, oil and water fractions at different C-ESP temperatures .....	79
<b>Figure 4.9</b> Energy recovered in the oil and water fractions at different C-ESP temperatures	80
<b>Figure 4.10</b> Total ion chromatograms of bio-oil samples from the three condensers for a C-ESP temperature of 70 °C .....	81
<b>Figure 4.11</b> Distribution of phenolic compounds from the pyrolytic vapors in oil and water fraction for a C-ESP temperature of 70 °C .....	82
<b>Figure 4.12</b> Yields of raw bio-oil, oil and water fractions at different pyrolysis temperatures .....	83
<b>Figure 4.13</b> Water content of raw bio-oil, oil and water fractions at different pyrolysis temperatures .....	84
<b>Figure 4.14</b> Heating value of raw bio-oil, oil and water fractions at different pyrolysis temperatures .....	85
<b>Figure 4.15</b> Energy recovered in oil fraction at different pyrolysis temperatures .....	86

**Figure 4.16** Heating value of dry bio-oil and other commercial fuels..... 87

## **1 Chapter 1: Introduction**

With depleting fossil fuel resources and increasing global warming, the production of fuels from renewable energy resources is growing in importance and is being stimulated by governments and the general public. Biomass represents one of the most promising renewable energy resources available on earth. Biomass is a generic term used for all organic matter that is derived from plants, trees, crops, algae, animals and animal wastes. Biomass is abundantly available and is a carbon neutral resource. Biomass is composed of three main constituents: cellulose, hemicellulose and lignin. Various processes have been developed to convert agricultural and forestry residual biomass into useful energy using bioconversion as well as thermo-chemical conversion technologies. In the recent past, fast pyrolysis of biomass has gained considerable interest as an efficient thermochemical conversion technology able to achieve high liquid yields from the thermal decomposition of biomass together with the production of other valuable co-products (bio-char and gas) (1, 2, 3).

### **1.1 Fast pyrolysis**

Pyrolysis is defined as the thermochemical decomposition of organic materials in the absence of oxygen. Pyrolysis of biomass results in three products: condensable vapors (liquids), non-condensable vapors (gases), char and ash (solids). Fast pyrolysis is the advanced process in which the yield of liquids can be maximized up to 75%, based on the type of the biomass. The main features of the fast pyrolysis process are:

1. Rapid heating and heat transfer rates, which require biomass with small particle size;

2. Pyrolysis reaction temperature of around 500°C to maximize the liquid yields, coupled with short residence time of the vapors inside the reactor of less than 2 seconds to avoid undesirable secondary cracking reactions;

3. Instant cooling of the condensable vapors to collect the liquid.

Maximum liquid yields are typically observed within the reactor temperature range of 450 to 550 °C and vapor residence times of 0.5 to 5 seconds. Various reactor types have been studied, but fluidized beds and circulating fluidized beds are more commonly used because they can be easily scaled-up and their operation is user friendly (1, 4).

The product stream from the fluidized bed reactor is a mixture of inert carrier gas, condensable vapors and aerosols, non-condensable gases, and solid char. Due to the presence of aerosols, complete recovery of the liquids cannot be achieved by simply cooling the product stream (1). Demisters are generally used to collect the aerosols, which may consist of specially designed impingers, liquid scrubbers or electrostatic precipitators (ESPs). A conceptual flow diagram of a biomass pyrolysis process is shown in Figure 1.1.

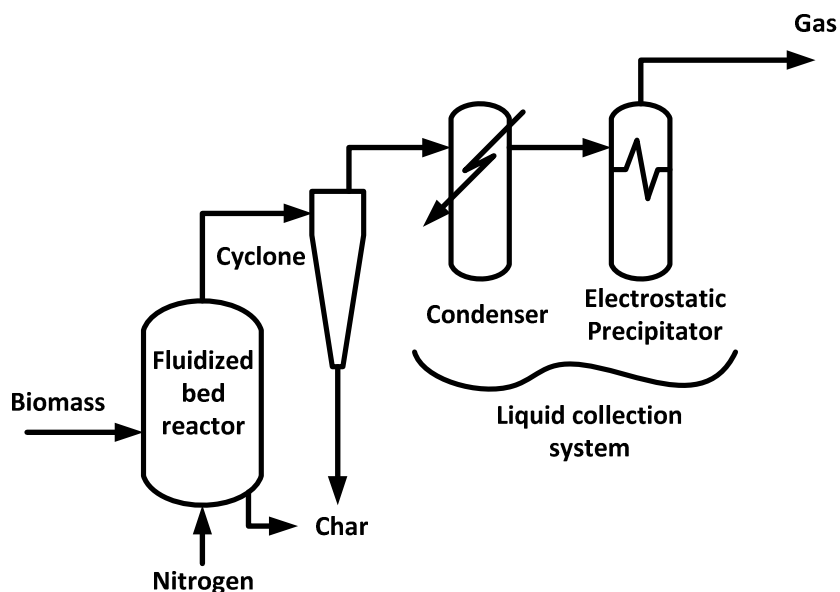


**Figure 1.1** Conceptual process flow diagram of fast pyrolysis process

## 1.2 Bio-oil

Fast pyrolysis liquid, also known as bio-oil, is a dark brown liquid, polar and highly oxygenated, which contains hundreds of chemical compounds with various functional groups, including organic acids, alcohol, aldehydes, aromatics, ketones, sugars, phenolics, and water. Bio-oils have tremendous potential to be used as fuel oil substitute and also to replace fossil fuel based chemicals. As a result of its high water and oxygen content, typical bio-oil has a heating value that is approximately 40% of the heating value of diesel. Apart from low heating value, bio-oils have other undesirable properties for fuel application such as high water content and immiscibility with fossil hydrocarbons, low thermal stability, high corrosiveness and high acidity (5, 6). Typical properties of bio-oil are compared with the properties of heavy fuel oil in Table 1.1.

**Table 1.1** Typical properties of wood pyrolysis bio-oil and heavy fuel oil (7)

<b>Physical property</b>	<b>Bio-oil</b>	<b>Heavy fuel oil</b>
Water content, wt%	15 – 30	0.1
pH	2.5	-
Specific gravity	1.2	0.94
Elemental composition, wt%		
Carbon	54 -58	85
Hydrogen	5.5 – 7	11
Oxygen	35 – 40	1
Nitrogen	0 – 0.2	0.3
ash	0 – 0.2	0.1
HHV, MJ/Kg	16 – 19	40
Viscosity (at 50 °C), cP	40 – 100	180
Solids, wt%	0.2 - 1	1

### 1.2.1 Heating value

The higher heating value (HHV) of bio-oils is in the range of 16 - 19 MJ/Kg depending on the type of biomass and the process conditions used for its production. The heating value of bio-oil is almost comparable to that of the raw biomass and is equivalent to approximately 40% of the heating value of fossil fuels. The low heating value of the bio-oil can be attributed to its high water concentration (15 – 30%) and high oxygen content (35 – 40%) (8).

### 1.2.2 Water content

High water content of bio-oils (15- 30%) is the result of two contributions: (a) the moisture content in the original biomass condenses in the oil; and (b) water that is produced by the pyrolysis reaction itself, as a result of dehydration reactions. The presence of water decreases the heating value and flame temperature of bio-oil. The high water content also makes the bio-oil more corrosive. Contrarily, it enhances the bio-oil flow characteristics by decreasing the viscosity of the oil (7, 8).

### 1.2.3 Acidity and Corrosiveness

Bio-oils contain substantial amounts of carboxylic acids, mostly acetic and formic acids, which lead to low pH values of 2 or 3. Because of the high acidity, bio-oils are corrosive to common metals such as carbon steel. The corrosiveness of bio-oils increases with increasing process temperature and with increasing water content (8).

### 1.2.4 Oxygen content

The presence of 35 – 40 wt% of oxygen in bio-oil leads to major differences in the properties of the bio-oils when compared to fossil fuels. The oxygen is present in most of the identified bio-oil compounds. The highest contributor to the oxygen content of the bio-oil is water, which is followed by groups of compounds such as hydroxyaldehydes, hydroxyketones, sugars, carboxylic acids, and phenolics. The high oxygen content of bio-oils results in a lower energy density, immiscibility with hydrocarbon fuels and instability (7).

### 1.2.5 Stability

The instability of bio-oils can be revealed in two ways:

1. Aging: a gradual increase in the viscosity of bio-oil while storage
2. Thermal instability: a rapid increase in the viscosity of bio-oil while heating, which leads to polymerization of certain compounds, phase separation and coke formation. Such thermal instability makes it impossible to implement conventional distillation technologies for the separation of the many valuable chemicals contained in the oil.

A rough sense of the impact of thermal instability may be gained by experimental findings that have shown that the increase in the molecular weight of a bio-oil after heating for one week at 80 °C was found to be same as when it was stored at room temperature for one year (9, 10).

### 1.3 Fractionation of bio-oils

Because of the undesirable properties discussed above, bio-oils have limited practical applications as raw products. The properties of the bio-oils, which are dependent on the chemical composition, can be considerably improved by fractionation of bio-oils. As in the case of conventional crude oil, distillation of bio-oil is not attractive because some of the constituents of bio-oil are highly reactive and, when heated, undergo thermal degradation that produces a solid residue (5). For this reason, fractional condensation of bio-oil vapors has been attracting attention as an effective downstream process to separate the constituents of bio-oils into different fractions (11-17).

In fractional condensation of bio-oil vapors, the product stream from the fast pyrolysis reactor is passed through a series of condensers maintained at different temperatures to allow the collection of liquid fractions of different physical and chemical properties in each condenser based on their dew point.

Williams and Brindle (11) utilized a series of seven condensers to separate single ring aromatic compounds from tire pyrolysis oil. They maintained the first three condensers at a single temperature (100, 150, 200 or 250 °C) to maximise the recovery of aromatics. The remaining four condensers were maintained at -70 °C to collect all of the oil. It was also reported that the usage of packing material (wire wool, pall rings) inside the first three condensers improved their oil yield.

Chen et al. (14) employed four stainless steel condensers in series followed by an electrostatic precipitator (ESP) to fractionate the bio-oil vapors from pine sawdust. Cooling water was circulated from the last condenser to the first condenser, to develop a small temperature gradient among the condensers. The ESP was placed at the end of the condenser train to collect the escaping aerosols. They found that the fractional condensation was useful to separate water and chemical compounds from the bio-oil.

Jendoubi et al. (15) used two condensers followed by an ESP to study the distribution of inorganic compounds in bio-oils. The first condenser was air cooled to collect the heavy phase and the second condenser was water cooled to recover the light oils. They found that the more than 60% of the inorganic compounds present in the whole raw bio-oil were contained in the oil collected by the ESP.

Westerhof et al. (16) utilized two counter-current spray condensers and an intensive cooler in series to fractionate the bio-oil into heavy and light fractions. They reported that the counter-current spray condensers are efficient in collecting the aerosols. The first condenser, maintained between 70 and 90 °C, collected heavy oil fractions, which contain 10% to 4% water and around 3% to 2% acetic acid. The heating value of the heavy oil fraction was in the range of 14 and 24 MJ/Kg on a wet oil basis. The light oil fraction collected in the second condenser contained around 10% acetic acid.

Pollard et al. (17) developed a five stage bio-oil collection system containing three condensers and two ESPs. One ESP was used between every two condensers to collect aerosols escaping the preceding condenser. The condensers were designed as shell and tube heat exchangers. The five stages of the collection system were maintained at different temperatures to enable the recovery of different classes of compounds at each stage of the condenser train. The water content of the first four bio-oil fractions was in the range of 7% to 15%. The heating value of the bio-oil fraction with 7% water content was 24 MJ/Kg.

#### **1.4 Aspen HYSYS**

Aspen HYSYS is a process modeling tool used for the simulation of chemical plants. HYSYS uses various thermodynamic models (Fluid Packages) to represent the phase equilibrium behaviour and energy level of pure components and mixture systems. HYSYS has been used in Chapter 2 to thermodynamically determine the maximum possible separation of the model compounds of the bio-oil.

## 1.5 Research Objectives

The work described in this thesis aims at investigating and optimizing a fractional condensation train which has the potential to improve the separation of bio-oil fractions and, consequently, their respective individual properties and uses.

In order to understand, improve and develop an effective fractional condensation system, Chapter 2 reviews the separation of model compounds of bio-oil using three condensers in series. Three model compounds, with different chemical and physical characteristics and representative of typical bio-oils, will be used for this study. The objective of this study is to condense primarily a single model compound in each condenser. The design of the fractional condensation train will be improved by comparing the experimental results with the theoretical results obtained by the HYSYS modeling software, for the same operating conditions.

Chapter 3 deals with the fractional condensation of real bio-oil vapors produced from the pyrolysis of birch bark. The aim of this study is to obtain dry bio-oil, i.e. with very low water content, from the pyrolysis of birch bark, in order to maximize its overall value (heating value and stability). The bio-oil samples will be analyzed for water content, heating value and the level of overall original energy recovered in the different fractions. The effect of pyrolysis temperature on the dry bio-oil yield and characteristics will also be investigated.

Chapter 4 deals with the fractional condensation of real bio-oil vapors produced from the pyrolysis of Kraft lignin. The aim of this study is to collect dry bio-oil from the pyrolysis of Kraft lignin, thus maximizing its value and stability as a potential source of

chemicals. The bio-oil samples will be analyzed for the water content, heating value, phenolics content, as well as the energy and phenolics recovered in the different fractions. The effect of reactor temperature on the dry bio-oil yield and characteristics will also be investigated.

## 1.6 References

- (1) Bridgwater AV, Meier D, Radlein D. An overview of fast pyrolysis of biomass. *Org Geochem* 1999 26 November 1998 through 27 November 1998;30(12):1479-1493.
- (2) Demirbas A. Combustion of biomass. *Energy Sources, Part A: Recovery, Utilization and Environmental Effects* 2007;29(6):549-561.
- (3) Briens C, Piskorz J, Berruti F. Biomass Valorization for Fuel and Chemicals Production – A Review. *International Journal of Chemical Reactor Engineering* 2008;6.
- (4) Bridgwater AV, Peacocke GVC. Fast pyrolysis processes for biomass. *Renewable & Sustainable Energy Reviews* 2000;4(1):1-73.
- (5) Bridgwater AV. Renewable fuels and chemicals by thermal processing of biomass. *Chem Eng J* 2003 3/15;91(2–3):87-102.
- (6) Mullen CA, Boateng AA. Chemical composition of bio-oils produced by fast pyrolysis of two energy crops. *Energy Fuels* 2008;22(3):2104-2109.
- (7) Czernik S, Bridgwater AV. Overview of applications of biomass fast pyrolysis oil. *Energy and Fuels* 2004;18(2):590-598.
- (8) Oasmaa A, Czernik S. Fuel oil quality of biomass pyrolysis oils - state of the art for the end users. *Energy and Fuels* 1999;13(4):914-921.
- (9) Oasmaa A, Kuoppala E. Fast pyrolysis of forestry residue. 3. Storage stability of liquid fuel. *Energy and Fuels* 2003;17(4):1075-1084.

- (10) Chaala A, Ba T, Garcia-Perez M, Roy C. Colloidal properties of bio-oils obtained by vacuum pyrolysis of softwood bark: Aging and thermal stability. *Energy and Fuels* 2004;18(5):1535-1542.
- (11) Williams PT, Brindle AJ. Temperature selective condensation of tyre pyrolysis oils to maximise the recovery of single ring aromatic compounds. *Fuel* 2003;82(9):1023-1031.
- (12) Oasmaa A, Sipilä K, Solantausta Y, Kuoppala E. Quality improvement of pyrolysis liquid: Effect of light volatiles on the stability of pyrolysis liquids. *Energy and Fuels* 2005;19(6):2556-2561.
- (13) Westerhof RJM, Kuipers NJM, Kersten SRA, Van Swaaij WPM. Controlling the water content of biomass fast pyrolysis oil. *Industrial and Engineering Chemistry Research* 2007;46(26):9238-9247.
- (14) Chen T, Deng C, Liu R. Effect of selective condensation on the characterization of bio-oil from pine sawdust fast pyrolysis using a fluidized-bed reactor. *Energy and Fuels* 2010;24(12):6616-6623.
- (15) Jendoubi N, Broust F, Commandre JM, Mauviel G, Sardin M, Lédé J. Inorganics distribution in bio oils and char produced by biomass fast pyrolysis: The key role of aerosols. *J Anal Appl Pyrolysis* 2011;92(1):59-67.
- (16) Westerhof RJM, Brilman DWF, Garcia-Perez M, Wang Z, Oudenhoven SRG, Van Swaaij WPM, et al. Fractional condensation of biomass pyrolysis vapors. *Energy and Fuels* 2011;25(4):1817-1829.
- (17) Pollard AS, Rover MR, Brown RC. Characterization of bio-oil recovered as stage fractions with unique chemical and physical properties. *J Anal Appl Pyrolysis* 2012;93:129-138.

## **2 Chapter 2: Fractional condensation of model compounds of bio-oil**

### **2.1 Introduction**

Bio-oils produced from fast pyrolysis of lignocellulosic biomass have potential to replace fossil fuel based chemicals. Bio-oil is a dark brown liquid that contains hundreds of chemical compounds of various functional groups, including organic acids, alcohols, aldehydes, aromatics, ketones, sugars and lignin derived phenolics. Bio-oils have limited practical applications due to their undesirable properties such as low thermal stability, high acidity, high corrosiveness and low heating value (1, 2).

Fractionation of bio-oils is required to increase their applicability and commercial value. Bio-oils cannot be distilled because some of their constituents are highly reactive and produce large quantities of solid residues upon heating (1). For this reason, fractional condensation of bio-oil vapors has been attracting attention as an effective downstream process to separate the constituents of bio-oils into different fractions (4-8).

In fractional condensation of bio-oil vapors, the product stream from the fast pyrolysis reactor is passed through a series of condensers maintained at different temperatures to enable the collection of liquid fractions of different physical and chemical properties in each condenser.

The product stream from the fast pyrolysis reactor is a mixture of fluidizing gas, vapors and aerosols. Due to the presence of aerosols, complete recovery of the bio-oil cannot be achieved by simply cooling the product stream (3). Therefore, demisters (impingers or electrostatic precipitators) are required to efficiently collect the aerosols.

Williams and Brindle (4) utilized a series of seven condensers to separate single ring aromatic compounds from tire pyrolysis oil. They maintained the first three condensers at a single temperature (100, 150, 200 or 250 °C) to maximize the recovery of aromatics. The remaining four condensers were maintained at -70 °C to collect all of the oil. It was also reported that the use of packing material (wire wool, pall rings) inside the first three condensers improved their oil recovery.

Chen et al. (5) employed four stainless steel condensers in series followed by an electrostatic precipitator (ESP) to fractionate the bio-oil vapors from pine sawdust. Cooling water was circulated from last condenser to first condenser to develop a small temperature gradient among the condensers. The ESP was placed at the end of the condenser train to collect the remaining aerosols.

Jendoubi et al. (6) used two condensers followed by an ESP to study the distribution of inorganic compounds in bio-oils. The first condenser was air cooled to collect the heavy phase and the second condenser was water cooled to recover the light oils.

Westerhof et al. (7) reported that counter-current spray condensers are efficient in collecting the aerosols. They used two counter-current spray condensers and an intensive cooler in series to fractionate the bio-oil into heavy and light fractions.

Pollard et al. (8) developed a five stage bio-oil collection system including three condensers and two ESPs. One ESP was used between every two condensers to collect aerosols escaping the preceding condenser. The condensers were designed as shell and tube heat exchangers. The five stages of the collection system were maintained at

different temperatures to enable the recovery of different classes of compounds at each stage of the condenser train. The five stage condenser train was followed by a glass wool filter to collect the remaining bio-oil.

As bio-oil is a complex mixture and its composition not fully known, it is not theoretically possible to calculate the extent of separation achievable with a fractional condensation train. In order to develop an effective fractional condensation system, the present study deals with the separation of model compounds of bio-oil using a condenser train. Three cyclonic condensers in series are used in this study to separate three model compounds from a mixture, representative of major classes of components present in the vapor and gas mixture exiting a typical biomass pyrolysis reactor.

Aspen HYSYS is a process modeling tool used for the simulation of chemical plants. HYSYS uses various thermodynamic models (Fluid Packages) to represent the phase equilibrium behaviour and energy level of pure components and mixture systems. HYSYS is employed to thermodynamically determine the required temperatures of the three condensers that would provide optimum separation of three model compounds. The practical efficiency of the fractional condensation train is estimated by comparing, for the same operating conditions, the experimental results with the results of the HYSYS simulation.

As water constitutes 10 to 30 wt % of total composition of bio-oil, water is selected as one of the model compounds (2). Glycerol and ethylene glycol are selected as two other representative model oxygenates for this study. The boiling points of the selected compounds are as follows: 290 °C for glycerol, 197.3 °C for ethylene glycol, and 100 °C

for water, to allow for good, theoretical separation through fractional condensation. The aim of this study is to condense most of the glycerol in the first condenser, most of the ethylene glycol in the second condenser, and most of the water in the final condenser.

## 2.2 Materials and methods

### 2.2.1 Continuous Feeding System

A positive pressure blow tank is used to pump the model compound mixture into 1 m stainless steel tubing of  $6.35 \times 10^{-3}$  m diameter. The tubing is positioned inside the HP 5890 GC oven, which provides the heat required for vaporization of liquid mixture passing through the tubing. The vapors exiting the coil are mixed with the continuous flow of heated nitrogen inside a T pipe fitting as shown in Figure 2.1. Before entering the oven, the nitrogen is heated to around 140 °C using the 400 W in-line air process heater (Omega AHP-5051). The temperature of the air process heater can be controlled by varying the voltage using an auto-transformer. The vapor and nitrogen mixture from the T pipe fitting flows on to the downstream condenser system. The temperature and pressure of the stream entering the condensers are continuously monitored using a K-type thermocouple and a liquid filled pressure gauge.

During most of the experimental runs, the input mixture in the blow tank was composed of the three model compounds in equal weight fractions. The weight of the blow tank was taken before and after each experiment. The flow rate of liquid mixture from the blow tank was maintained at around 8 to 10 g/min. The liquid flow rate was controlled by regulating the pressure of the blow tank and also by changing the capillary connecting the blow tank and  $6.35 \times 10^{-3}$  m diameter tubing. The flow rate of the nitrogen

was maintained at 23 L/min using a sonic nozzle of  $1 \times 10^{-3}$  m diameter. The nitrogen pressure upstream of the sonic nozzle was maintained at  $2.76 \times 10^5$  Pa to achieve the flow rate of 23 L/min. Each experiment lasted 15 minutes.

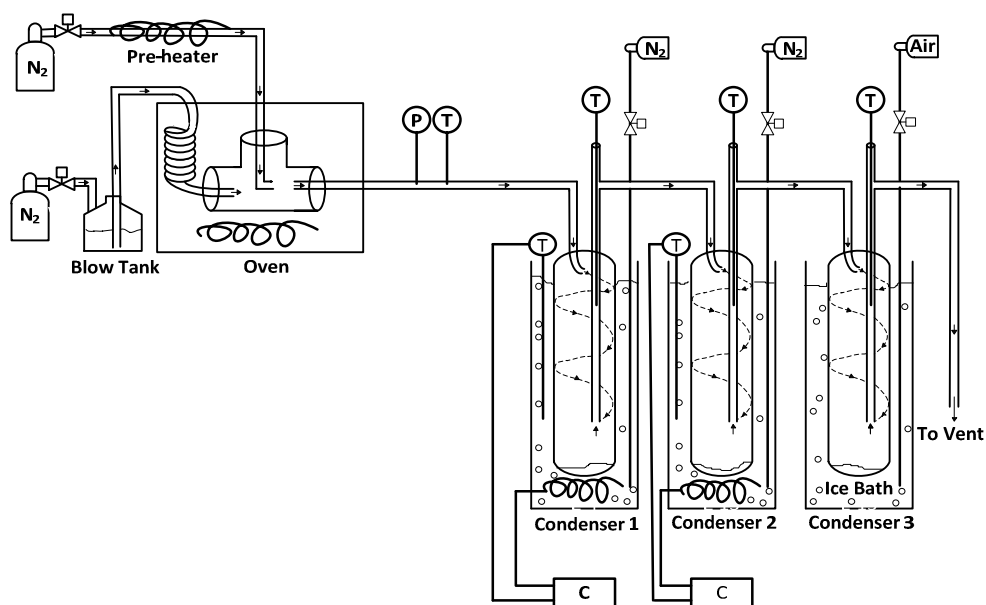


**Figure 2.1** Process Flow Diagram of model compounds feeding system and condenser train

### 2.2.2 Condensing System

The condenser train consists of three stainless steel cyclonic condensers connected in series. As shown in Figure 2.1, the mixture of vapors and gases enters each condenser and is immediately directed to the condenser wall with a  $90^\circ$  elbow. This nearly tangential entry forces the vapors and gases to spin, providing good agitation and heat transfer and driving the condensed liquid droplets against the wall through cyclonic action. Each compact condenser can be weighed before and after each run to obtain an accurate liquid collection yield. It can also be easily taken apart and any oil deposit on the wall can be recovered with a specially designed scraper (9).

To maintain the condensers at different temperatures, each condenser is immersed in a separate temperature-controlled bath. As the first condenser is intended to concentrate glycerol, the temperature of the first condenser has to be higher than the dew point temperatures of ethylene glycol and water. The heat transfer fluid used in the first bath is Duratherm G, which has a flash point of 223 °C. Paraffin oil is used as heat transfer fluid in the second bath. With paraffin oil, the second condenser can be maintained at a maximum temperature of around 193 °C. The third condenser, which has to recover all the non-condensable vapors, is placed in an ice water bath. High temperature cartridge heaters, located at the bottom of first and second baths, maintain each of the bath fluids at the desired temperature. The temperatures of the cartridge heaters are controlled using Watlow series C on-off temperature controllers. To ensure the uniformity of temperature along the entire length of the condensers and also for good heat transfer from the walls of the condensers, nitrogen is bubbled at a very low flow rate in the first and second baths, and air is bubbled in the ice water bath. The temperature of the stream leaving each condenser is constantly recorded using K-type thermocouple placed in the condenser outlet tubing.

To capture the aerosols escaping from the first condenser, two types of impingement surfaces are tested inside condenser 1: aluminum fan blades, and stainless steel wool. These mist collectors are mounted on the outlet tubing of the first condenser.

### 2.2.3 Determination of the condensate composition

The weight fraction of water in the condensed liquid was obtained by using a volumetric Karl Fischer titrator. The weight fractions of the remaining two compounds in the condensate were then calculated by solving the following two linear equations:

1. Weight fraction equation:

$$X_{\text{Glycerol}} + X_{\text{Ethylene Glycol}} + X_{\text{Water}} = 1 \quad (1)$$

where  $X$  is the weight fraction.

2. Liquid mixture density equation:

$$\rho_{\text{condensate}} = (X_{\text{Glycerol}} \times \rho_{\text{Glycerol}}) + (X_{\text{Ethylene Glycol}} \times \rho_{\text{Ethylene Glycol}}) + (X_{\text{Water}} \times \rho_{\text{Water}}) \quad (2)$$

where  $\rho_{\text{condensate}}$  = density of condensate,

and  $\rho_{\text{Glycerol}}$ ,  $\rho_{\text{Ethylene Glycol}}$ ,  $\rho_{\text{Water}}$  are the densities of the pure compounds.

The densities of the condensate and pure compounds were determined with an SVM 3000 Anton Paar viscometer.

## 2.3 Experimental results and discussion

The study proceeded through the following steps:

1. HYSYS simulation to select the best condenser temperatures;
2. Checking that the heat transfer from the condenser wall to the vapors was sufficiently good to condense the vapors and reach nearly thermal equilibrium of the exiting vapors with the condenser bath temperature;

3. Verifying that the mixing of the vapors within the condensers was sufficiently good to ensure that all vapors exited the condenser at the same temperature;
4. Modifying the condensers so that their performance would approach the theoretical performance.

### 2.3.1 HYSYS simulation to select condenser temperatures

The schematic in Figure 2.1 is simulated using Aspen HYSYS 2006 with the PRSV fluid package. The PRSV equation of state is selected as the fluid package because it can manage non-ideal systems with accuracies as good as activity coefficient models (10). In HYSYS, a flash separator has been used to represent each cyclonic condenser. A flash separator allows the vapor and liquid to attain thermodynamic equilibrium, as they are separated. Using HYSYS, the operating temperatures of the first and second condensers were selected by giving equal weightage to both the yield and purity of the compound being separated. The variation in the yield and purity of the compound being separated with the condenser temperature is shown in Figure 2.2 and Figure 2.3. From Figure 2.2, the temperature range of 140 to 160 °C is selected as optimum for condenser 1, for the recovery of glycerol. From Figure 2.3, the temperature range of 70 to 90 °C is selected as optimum for condenser 2, for the condensation of ethylene glycol.

Experiments were performed with the temperature of the first condenser at 140 and 160 °C. The second condenser was tested at temperatures of 80 and 90 °C.

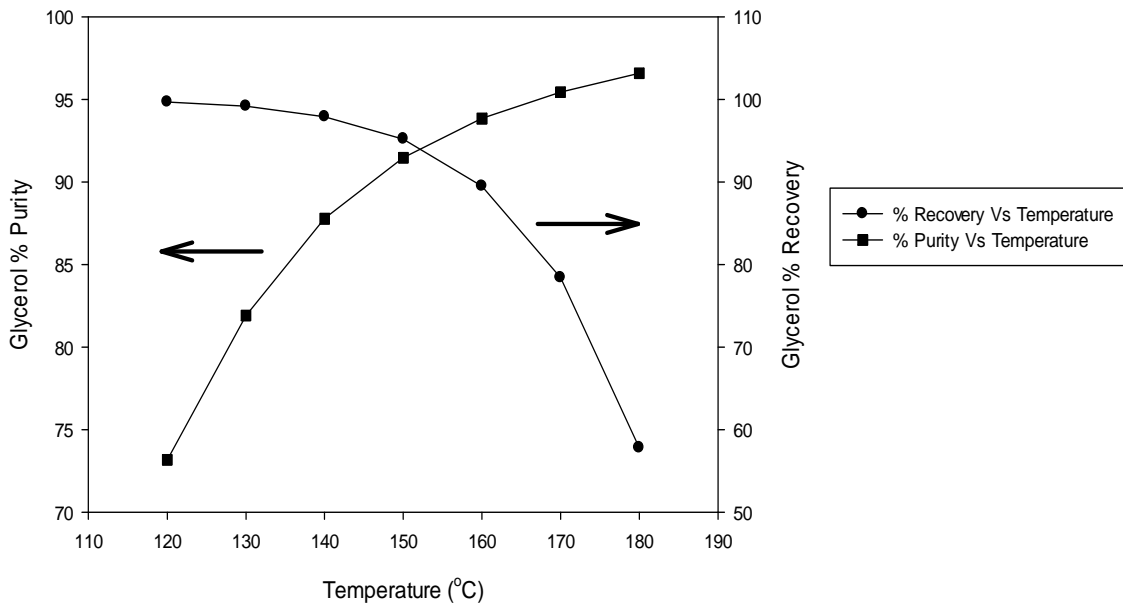


**Figure 2.2** Glycerol % Recovery and % Purity as functions of Temperature of Condenser 1, as predicted with HYSIS

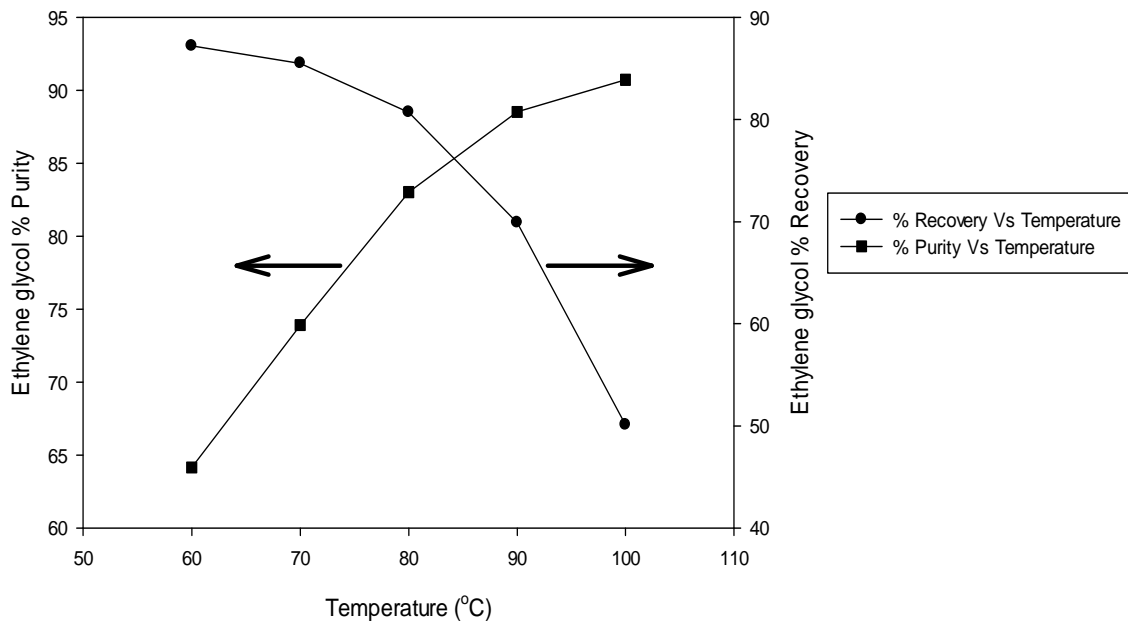


**Figure 2.3** Ethylene glycol % Recovery and % Purity as functions of Temperature of Condenser 2, as predicted with HYSIS

### 2.3.2 Heat transfer in condensers

At each stage of the condenser train, the gas and vapor mixture stream has to be cooled down by 60 to 80 °C. To achieve the targeted cooling, good heat transfer in the

cyclonic condensers is crucial. As the temperature of the heat transfer fluid in the condenser bath is maintained using a controller, the heat transfer performance of a condenser can be validated by comparing the temperature of the heat transfer fluid in the condenser bath with the temperature recorded at the condenser outlet ( $T_{\text{exit}}$ ). The temperature profiles along the condenser train for one of the experimental runs is shown in Figure 2.4. In this particular experimental run, the baths of first and second condensers were maintained at 140 and 80 °C, respectively, while the temperature of the vaporized mixture entering condenser 1 varied between 200 and 223 °C. Over the 15 minutes run, the average temperatures ( $T_{\text{exit}}$ ) at the outlets of condensers 1 and 2 were 144 and 87 °C respectively. These average temperatures are quite close to the target temperatures set in the heating baths, which indicate that the heat transfer in both the condensers is nearly perfect.

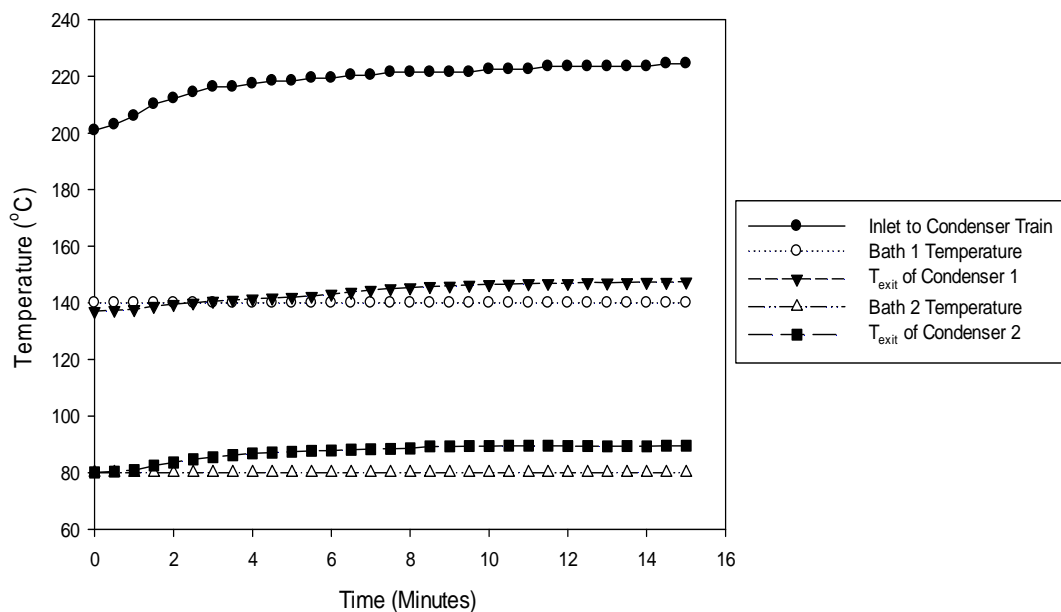


**Figure 2.4** Temperature Profile along the Condenser Train

Ten experiments were carried out under different operating conditions in order to understand the factors affecting the fractional condensation. The operating conditions of all the experiments are shown in the Table 2.1 and Table 2.2. Some of the experiments were repeated to verify that the results were reproducible. In all these experiments, the main focus was to maximize the separation efficiency. To check the efficiency of the fractional condensation train, experimental results are compared with the results of the HYSYS simulation in terms of the following features:

1. Good mixing to achieve condensation of the whole stream; and
2. Yield of condensers.

**Table 2.1** Operating conditions used in all the experiments carried out using liquid mixture consisting of three model compounds (Glycerol: Ethylene glycol: Water = 0.33 wt%: 0.33 wt%: 0.33 wt%)

S. No	Liquid Flow rate (g/min)	N <sub>2</sub> Flow rate (L/min)	Bath 1 Temperature (°C)	Bath 2 Temperature (°C)	Mist Collector Used in Condenser 1
1	9.2	10	160	100	-
2	9.4	14	160	100	-
3	8.7	23	160	100	-
4	8.4	23	140	80	-
5	8.1	23	140	80	One Fan
6	8.1	23	140	80	Stainless Steel Wool

**Table 2.2** Operating conditions used in all the experiments carried out using liquid mixture consisting of two model compounds (Ethylene glycol: Water = 0.66 wt%: 0.34 wt%)

<b>S. No</b>	<b>Liquid Flow rate (g/min)</b>	<b>N<sub>2</sub> Flow rate (L/min)</b>	<b>Bath 1 Temperature (°C)</b>	<b>Bath 2 Temperature (°C)</b>	<b>Mist Collector Used in Condenser 1</b>
1	9.4	23	100	100	-
2	9	23	100	100	One Fan
3	10.2	23	100	100	Two Fans
4	9.3	23	100	100	Three Fans

### 2.3.3 Mixing and condensate composition

Good mixing of the vapors inside the condensers is essential to achieve the required condensation. In other words, mixing inside each of the condensers will ultimately determine the composition of its condensate. If the mixing inside the condenser is good, then all the vapors exit the condenser at the same temperature, and the composition of the condensate will be approximately the same as the composition predicted by HYSYS.

For most of the experiments, the yield of first condenser was lower than the yield predicted by HYSYS. As the experimental yield of the first condenser is not matching with that of HYSYS, it can be easily concluded that the experimental composition of the input streams to condensers 2 and 3 would also be different from the composition predicted with HYSYS. For this reason, the initial part of the study is focused on the first condenser, for which the composition of its input stream was exactly the same as that predicted with the HYSYS simulations.

### 2.3.3.1 Condensate composition at different nitrogen flow-rates

To verify that there was good mixing of the vapors inside the condenser, at various nitrogen flow rates, experiments were carried out at three selected nitrogen flow rates of 10, 14 and 23 L/min. During all the experiments, the liquid flow rate was maintained at around 8.7 to 9.4 g/min and the first condenser temperature was set at 160 °C. For different nitrogen flow rates, the composition of the condensate collected in condenser 1 and the corresponding HYSYS results are shown in Figure 2.5. In all cases, the experimental composition is practically identical to the composition estimated by HYSYS. This confirms that the mixing of the vapors was excellent in the cyclonic condensers.

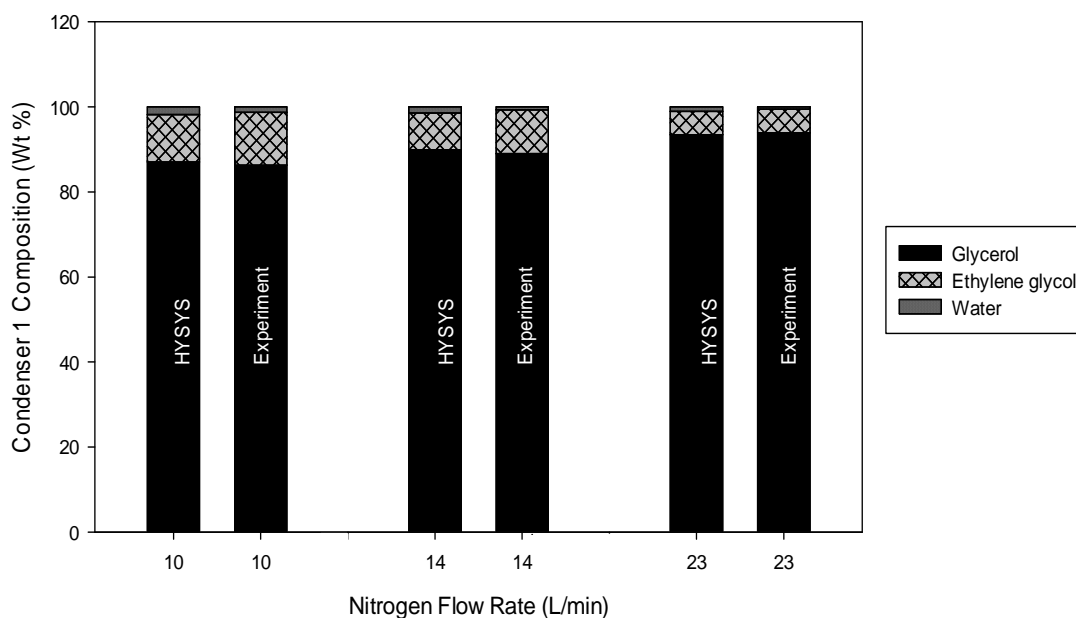


**Figure 2.5** Composition of condensate in Condenser 1 at different nitrogen flow rates

### 2.3.3.2 Condensate composition at different temperatures of condenser 1

The influence of the temperature of condenser 1 on the composition of the condensate is shown in Figure 2.6. The condenser temperature reported in Figure 2.6 is the average temperature of the condenser 1 over the 15 minutes experimental run. In both experiments, the nitrogen and liquid flow rates were kept constant at 23 L/min and 8.4 to 8.7 g/min, respectively. As shown in the Figure 2.6, the condensate composition in condenser 1 is the same as the HYSYS predictions at the different temperatures of the first condenser.

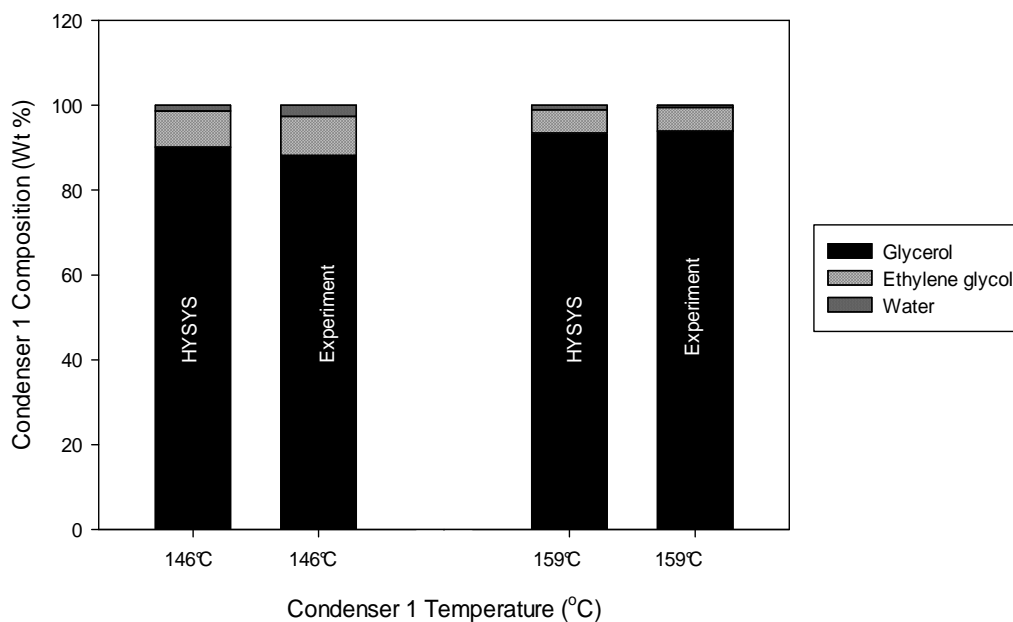


**Figure 2.6** Composition of condensate in Condenser 1 at different condenser temperatures

From the above results, it can be concluded that there exist a nearly perfect heat transfer and mixing inside the cyclonic condensers.

#### 2.3.4 Yield of Condensers

Although the composition of the liquid collected by the first condenser matched the theoretical composition predicted by HYSYS, the yield of condenser 1 is much lower than the yield calculated by HYSYS. Table 1 shows that the mass of liquid collected in the first condenser was always much lower than the HYSYS prediction. This is consistent with a fraction of the condensed liquid escaping the condenser as a fine mist (aerosol).

**Table 2.3** Comparison of mass of liquid collected in condenser 1 with HYSYS predictions for different experimental conditions

S.No	N <sub>2</sub> Flow rate (L/min)	Average Temperature of Condenser 1 (°C)	Mass of liquid collected in Condenser 1 (grams)	
			HYSYS	Experiment
1	14	160	50.4	35
2	23	159	41.9	23.5
3	23	146	44.8	35.5

As the aerosols escape from condenser 1, the input stream to condensers 2 and 3 is not comparable to that of HYSYS. For this purpose, only the yield of condenser 1 is taken into consideration in the further discussion about the yield of condensers. For condition 3 listed in Table 2.3, the experimental liquid yield of three condensers compared to that simulated with HYSYS is shown in Figure 2.7. Figure 2.7 shows that the flow rate escaping the final condenser is much larger than predicted, which is also consistent with losses of a fine aerosol mist.

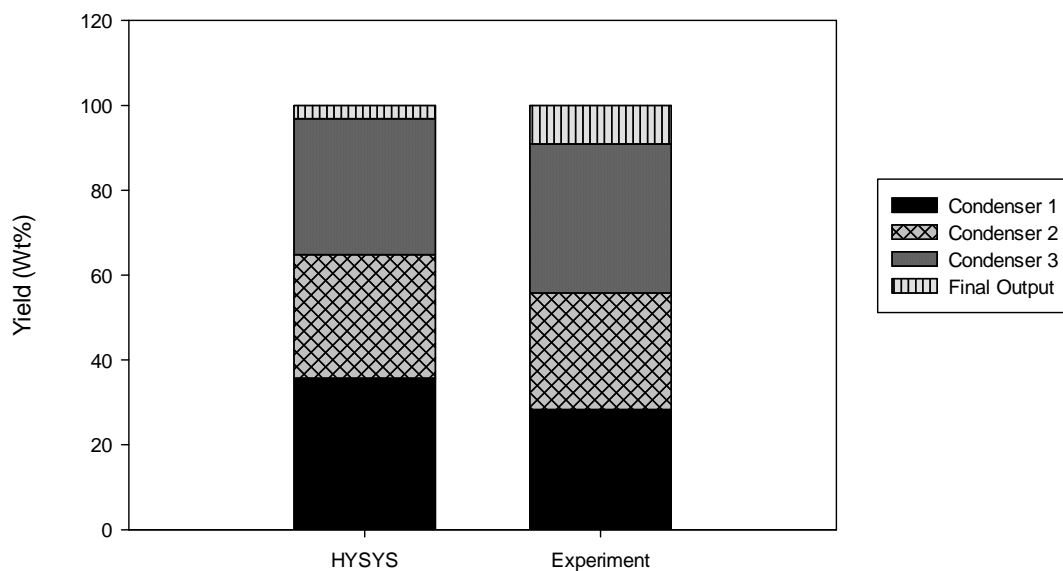


**Figure 2.7** Comparison of experimental yields of three condensers to HYSYS results

#### 2.3.4.1 Quantification of liquid lost as mist

The aerosols escaping from the first condenser need to be captured to match the experimental yield and the HYSYS yield and increase the separation efficiency of the condenser train. To quantify the mist lost from the first condenser, the following formula has been used:

$$\% \text{ of liquid lost from condenser 1} = \left( \frac{M_{L,HYSYS} - M_{L,Measured}}{M_{L,HYSYS}} \right) * 100 \quad (3)$$

where:

$M_{L,HYSYS}$  = Mass of liquid collected in condenser 1 as predicted by HYSYS

$M_{L,Measured}$  = Actual mass of liquid experimentally collected in condenser 1

#### 2.3.4.2 Effect of Nitrogen Flow rate

As discussed earlier in the mixing subsection, three nitrogen flow rates of 10, 14 and 23 L/min were used. During these experiments, the temperature of the bath of condenser 1 was set at 160 °C and the liquid flow rate was maintained at 8.7 to 9.4 g/min. Fig. 8 shows the weight fraction of liquid lost as mist from the first condenser at different nitrogen flow rates. From Figure 2.8, it is apparent that there is a significant increase in the mist losses from condenser 1 with increasing nitrogen flow rate.

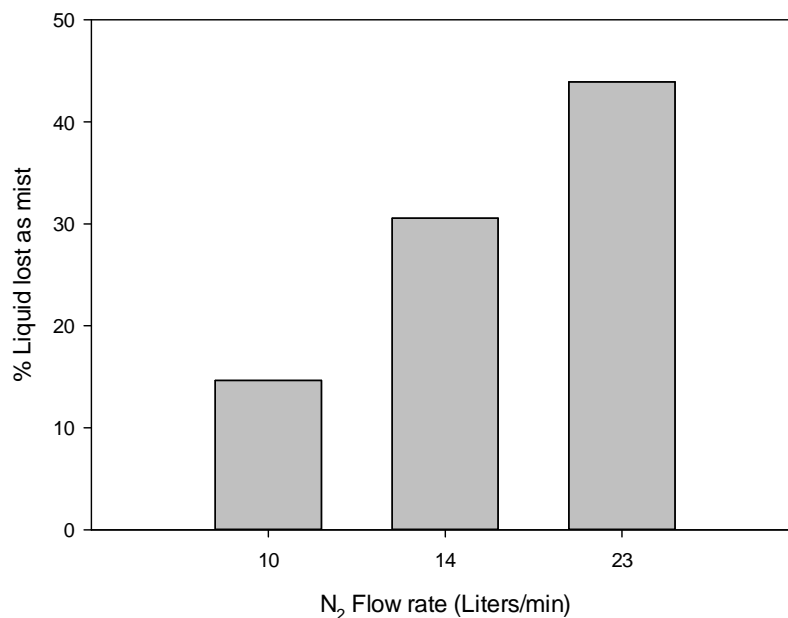


**Figure 2.8** Effect of nitrogen flow rate on mist collection in first condenser

#### 2.3.4.3 Effect of Condenser Temperature

Two experiments were performed with condenser 1 maintained at different temperatures to check the effect of condenser temperature on the mist collection. During these runs, the nitrogen flow rate was kept constant at 23 L/min and the liquid flow rate

was maintained at 8.4 to 8.7 g/min. Figure 2.9 shows the mist losses from condenser 1 at the average temperatures of 146 and 159 °C: as the temperature of the condenser increases, the mist collection becomes more difficult. The reason for this is that, as the temperature increases, the surface tension of the condensed liquid decreases, which reduces the droplet size and facilitates the formation and loss of fine aerosols.

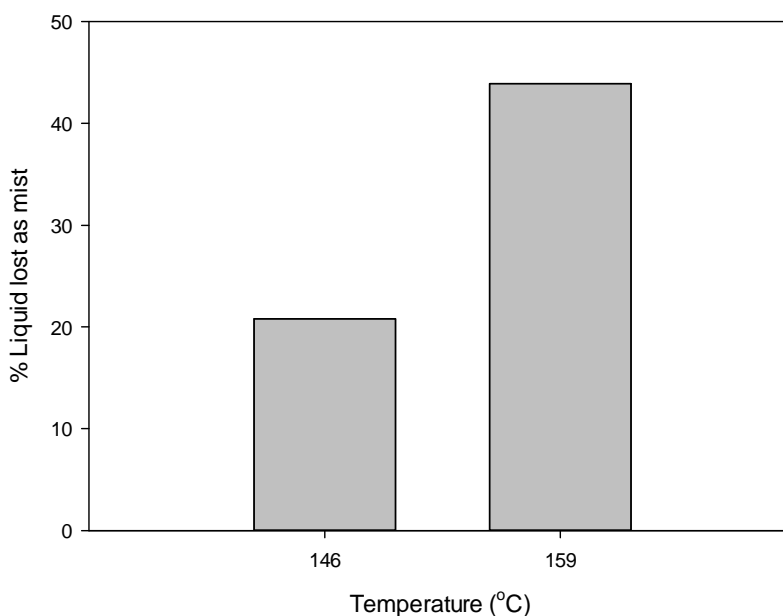


**Figure 2.9** Effect of temperature on mist collection in first condenser

#### 2.3.4.4 Effect of mist collectors

Aluminum fan blades and stainless steel wool were used in condenser 1 to capture the aerosols. Initially, a two-component mixture consisting of 66% ethylene glycol and 34% water was used to check the effectiveness of the aluminum fan blades in capturing the mist of ethylene glycol escaping from condenser 1. For these experiments, the average temperature of condenser 1 was around 110 °C; liquid flow rate and nitrogen

flow rate were kept at 9 to 10.2 g/min and 23 L/min, respectively. Experiments were performed without any fan and with one fan, two fans and three fans. Figure 2.10 shows that the best mist capture was achieved with one fan.

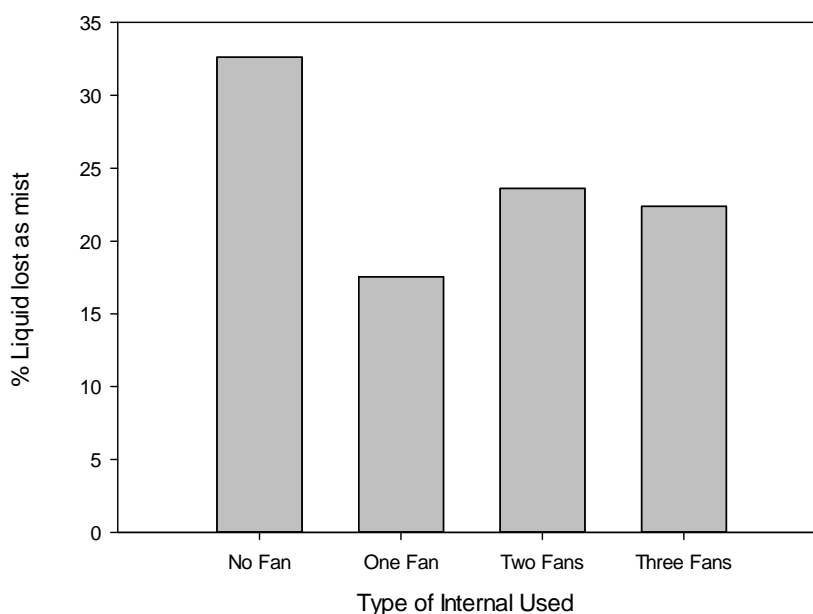


**Figure 2.10** Effect of aluminum fan blade on mist collection in first condenser

After achieving positive results with a two-component mixture, experiments were carried out with the original three-component mixture with the aim of decreasing the amount of glycerol aerosols escaping from condenser 1. In this case, one aluminum fan blade and stainless steel wool were used as mist collectors in the first condenser. For these experiments, nitrogen and liquid flow rates were maintained at 23 L/min and 8.1 to 8.4 g/min, respectively. The average temperature of the condenser 1 was around 145 °C. The performance of mist collectors can be seen in Figure 2.11.

Contrary to two component mixture, aluminum fan blades increased the amount of glycerol aerosols escaping from condenser 1. But, stainless steel wool proved to be a good mist collector for the glycerol at 145 °C. The increase in condenser 1 temperature from 110 °C (for the case of two component mixture) to 145 °C (for the three-component mixture) is the main reason that aluminum fan blades failed in capturing the aerosols of glycerol. As the temperature of condensation increases, the overall surface tension of the liquid mixture decreases, thus reducing the droplet size. For this reason, more effective impingement surfaces are required at higher condensation temperatures to capture the aerosols.

In the case of aluminum fan blades, the increase in the weight fraction of glycerol aerosols lost is probably caused by the atomization and re-entrainment of the condensed liquid droplets collected on the fan blades. The fan collects large liquid droplets that form a liquid film on the fan surface, and the gas flow shears off, from the liquid on the fan edge, fine droplets that are even more difficult to collect in the condenser.

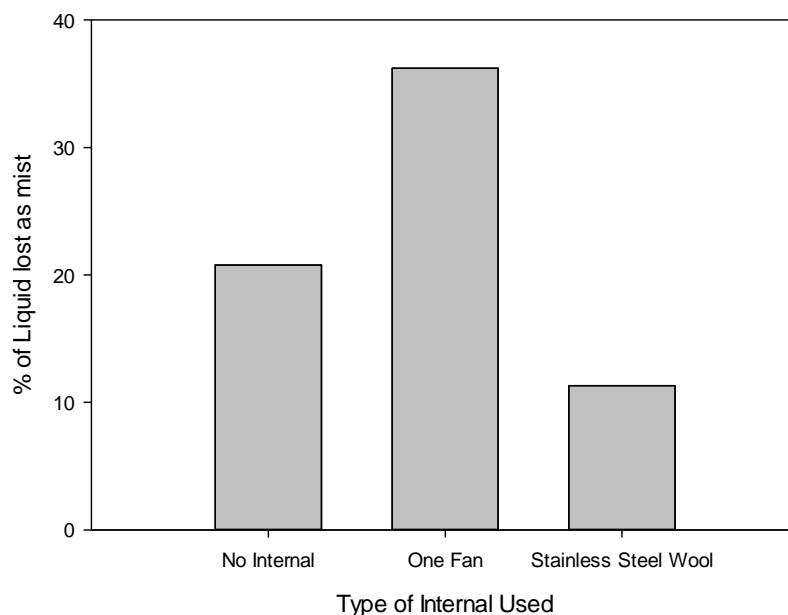


**Figure 2.11** Effect of internals on mist collection in first condenser

The highest efficiency of separation that can be achieved with the fractional condensation process is the condition where both the purity and the yield of the separated compounds are matching the theoretical predictions. In order to rank the efficiency of separation achieved with different mist collectors, two performance indices are defined to quantify the purity and yield:

1. Purity Performance Index ( $P_{purity}$ ): it indicates the purity of the compounds experimentally separated in the fractional condensation process when compared to that of HYSYS. If the value of  $P_{purity}$  is 1, the purity of compounds separated is exactly the same as the purity predicted by HYSYS. As the value of  $P_{purity}$  decreases, it indicates that the purity of the separated compounds is declining when compared to that simulated with HYSYS. In the case of the

model compound mixture consisting of three components, the two valuable compounds, glycerol and ethylene glycol, need to be separated from water. The purity performance index,  $P_{purity}$  is therefore given by:

$$P_{purity} = 1 - \sqrt{\left(\frac{WF_G - WF_{G\ HYSYS}}{WF_{G\ HYSYS}}\right)_{Condenser\ 1}^2 + \left(\frac{WF_{EG} - WF_{EG\ HYSYS}}{WF_{EG\ HYSYS}}\right)_{Condenser\ 2}^2}$$

(4)

where  $WF_G$  is the experimental weight fraction of glycerol;  $WF_{G\ HYSYS}$  is the weight fraction of glycerol according to HYSYS;  $WF_{EG}$  is the experimental weight fraction of ethylene glycol; and  $WF_{EG\ HYSYS}$  is the weight fraction of ethylene glycol according to HYSYS.

2. Yield Performance Index ( $P_{yield}$ ):  $P_{yield}$  will denote the yield of glycerol in the first condenser and of ethylene glycol in the second condenser when compared to those predicted with HYSYS. The yield performance index,  $P_{yield}$  is given by:

$$P_{yield} = 1 - \sqrt{\left(\frac{M_G - M_{G\ HYSYS}}{M_{G\ HYSYS}}\right)_{Condenser\ 1}^2 + \left(\frac{M_{EG} - M_{EG\ HYSYS}}{M_{EG\ HYSYS}}\right)_{Condenser\ 2}^2}$$

(5)

where  $M_G$  is the experimental mass of glycerol;  $M_{G\ HYSYS}$  is the mass of glycerol according to HYSYS;  $M_{EG}$  is the experimental mass of ethylene glycol; and  $M_{EG\ HYSYS}$  is the mass of ethylene glycol according to HYSYS.

The values of two performance indices, purity and yield, in presence of different mist collectors are shown in Table 2.4.

**Table 2.4** Performance indices in presence of different mist collectors for the three-component model mixture

<b>Type of Mist Collector</b>	<b><math>P_{purity}</math></b>	<b><math>P_{yield}</math></b>
Without any mist collector	0.87	0.72
Aluminum fan blade	0.81	0.59
Stainless steel wool	0.93	0.80

Table 2.4 shows that the stainless steel wool gave the best results in terms of both purity and yield. Therefore, it can be concluded that the best separation of the three-component model mixture is achieved with the help of a stainless steel wool section placed in the first condenser. In this experiment, the average temperatures recorded for the three condensers were in the following sequence: 144, 87 and 18 °C. The best individual component yields attained in the three condensers as against the HYSYS predictions are shown in Figure 2.12.

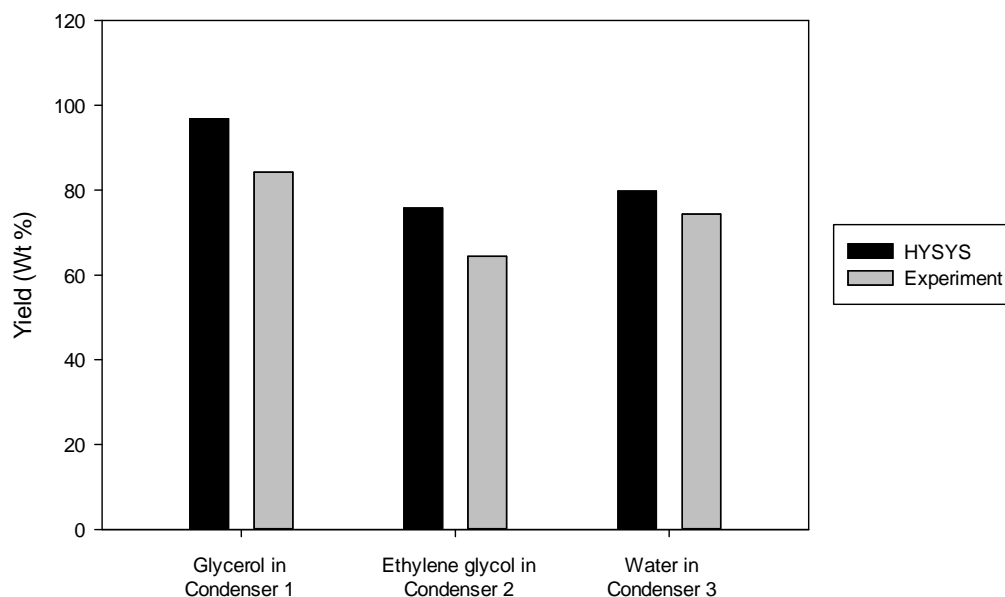


**Figure 2.12** Comparison of the yields of individual components predicted by HYSYS to the yields achieved with stainless steel wool demister in the first condenser

## 2.4 Conclusions

The fractional condensation of a mixture of three bio-oil model compounds from a vapor and carrier gas stream has been investigated with the help of a series of three condensers maintained at different temperatures. The theoretical results predicted by the HYSYS modeling tool were used as reference to determine and benchmark the practical performance of the fractional condensation train. The effects of carrier gas flow rate and of condenser temperature on the mist collection in the first condenser have been determined. A stainless steel wool demister proved to provide a good impingement surface to capture the aerosols of glycerol escaping from the first condenser. The impact of the condenser temperature on the surface tension of the liquid should be considered as it affects the size of the mist droplets and, consequently, their potential re-entrainment and loss from each condenser.

## 2.5 References

- (1) Bridgwater AV. Renewable fuels and chemicals by thermal processing of biomass. *Chem Eng J* 2003 3/15; 91(2–3): 87-102.
- (2) Mullen CA, Boateng AA. Chemical composition of bio-oils produced by fast pyrolysis of two energy crops. *Energy Fuels* 2008; 22(3): 2104-2109.
- (3) Bridgwater AV, Meier D, Radlein D. An overview of fast pyrolysis of biomass. *Org Geochem* 1999 26 November 1998 through 27 November 1998; 30(12): 1479-1493.
- (4) Williams PT, Brindle AJ. Temperature selective condensation of tyre pyrolysis oils to maximise the recovery of single ring aromatic compounds. *Fuel* 2003; 82(9): 1023-1031.
- (5) Chen T, Deng C, Liu R. Effect of selective condensation on the characterization of bio-oil from pine sawdust fast pyrolysis using a fluidized-bed reactor. *Energy and Fuels* 2010; 24(12): 6616-6623.
- (6) Jendoubi N, Broust F, Commandre JM, Mauviel G, Sardin M, Lédé J. Inorganics distribution in bio oils and char produced by biomass fast pyrolysis: The key role of aerosols. *J Anal Appl Pyrolysis* 2011; 92(1): 59-67.
- (7) Westerhof RJM, Brilman DWF, Garcia-Perez M, Wang Z, Oudenhoven SRG, Van Swaaij WPM, et al. Fractional condensation of biomass pyrolysis vapors. *Energy and Fuels* 2011; 25(4): 1817-1829.

(8) Pollard AS, Rover MR, Brown RC. Characterization of bio-oil recovered as stage fractions with unique chemical and physical properties. *J Anal Appl Pyrolysis* 2012; 93: 129-138.

(9) Xu R, Ferrante L, Briens C, Berruti F. Flash pyrolysis of grape residues into biofuel in a bubbling fluid bed. *J Anal Appl Pyrolysis* 2009; 86(1): 58-65.

(10) <http://www.aspentech.com/hysys/>

### **3. Chapter 3: Fractional condensation of bio-oil vapors produced from birch bark pyrolysis**

#### **3.1 Introduction**

With rising energy requirements and gradually depleting fossil fuel resources, the interest for the production of fuels from biomass residues and wastes has been increasing. Various thermal processes have been developed to produce useful energy from different kinds of biomass residues. In the recent past, fast pyrolysis has been gaining immense interest because of its ability to achieve high liquid yields of up to 75%, based on the type of biomass, through the rapid thermal decomposition of lignocellulosic biomass in the absence of oxygen. Fast pyrolysis liquid, also called bio-oil, is a complex mixture of oxygenated hydrocarbons. A typical bio-oil has a higher heating value of around 17 MJ/kg, which is about 40% of the heating value of diesel. The relatively low heating value of the bio-oil can be attributed to its high water concentration (typically in the range between 15 and 30 wt%) and to the high oxygen content (35 – 40 wt%). Apart from their low heating value, bio-oils have other undesirable properties for fuel applications such as low thermal stability, high corrosiveness and high acidity. The upgrading of bio-oils is essential to convert bio-oils into stable liquid fuels (1, 2).

The energy density, corrosiveness and the phase stability of the bio-oils could be greatly improved by decreasing the water content of the bio-oils. The distillation of bio-oil is not attractive as some of its components are thermally sensitive, degrade and produce solid residues upon heating to temperatures greater than 100 °C (1). Recently, fractional condensation of the bio-oil vapors has been receiving increasing attention by

researchers to separate bio-oil constituents (3-6). In the fractional condensation process, the bio-oil vapor stream exiting the fast pyrolysis reactor is passed through a series of condensers maintained at different, gradually decreasing temperatures to enable the collection of liquid fractions of different physical and chemical properties in each condenser.

Westerhof et al. (5) utilized two counter-current spray condensers and an intensive cooler in series to fractionate the bio-oil into heavy and light fractions. The first condenser, maintained between 70 and 90 °C, collected heavy oil fraction, which contains 10% to 4% water and around 3% to 2% acetic acid. The heating value of the heavy oil fraction was in the range of 14 and 24 MJ/Kg on a wet oil basis. The light oil fraction collected in the second condenser contained around 10% acetic acid.

Pollard et al. (6) developed a five stage bio-oil collection system to enable the recovery of different classes of compounds at each stage of the condenser train. The water content of the first four bio-oil fractions was in between 6.6 to 14.8 wt%. These four oil fractions recovered 85% of the total bio-oil energy. The condensing system used three condensers and two electrostatic precipitators (ESPs). They used one ESP between every two condensers to collect aerosols escaping the preceding condenser. The condensers were designed as shell and tube heat exchangers.

The aim of the present study is to obtain dry bio-oil, i.e. with very low water content, from the pyrolysis of birch bark. Birch bark is pyrolyzed in a bubbling fluidized bed and the resulting bio-oil vapors are fractionated using a three-condensers train to obtain a dry bio-oil. This study uses a fractional condensation train that had been

optimized with model compounds, described in Chapter 2. The effect of reactor temperature on the dry bio-oil yield and characteristics will also be investigated.

## **3.2 Materials and methods**

### **3.2.1 Materials**

Birch bark was used as the feedstock and pyrolyzed using the ICFAR bubbling bed pyrolysis pilot plant (8, 9). To facilitate the continuous feeding using the ICFAR slug injector (7), the birch bark was ground to a particle size of about 1 mm prior to being fed into the bubbling bed reactor. The bulk density and the higher heating value of the resulting birch bark powder were  $200 \text{ kg/m}^3$  and  $22 \text{ MJ/kg}$ , respectively.

Inert silica sand with a Sauter-mean diameter of  $180 \text{ }\mu\text{m}$  was used as the bed material in the bubbling fluidized bed. The bed mass was  $1.5 \text{ kg}$ .

Nitrogen was used as the inert fluidization gas. Nitrogen was also the carrier gas for the injection of birch bark powder slugs into the bubbling bed using periodic gas pulsations.

### **3.2.2 Bubbling fluidized bed setup**

The fluid bed reactor is made of Inconel 600,  $0.075 \text{ m}$  in diameter, with a  $0.65 \text{ m}$  long cylindrical section (8). The reactor is heated by three radiative electric heaters, covering both the dense sand bed and the freeboard sections. The heaters are independently controlled using Watlow PID digital controllers, to set a constant temperature profile along the axis of the reactor. The temperature feedback for the

Watlow controllers is provided through the type K thermocouples placed within the bed at the same height as the heaters. The fluidization gas (nitrogen) enters the bed through the perforated distributed plate located at the bottom of the reactor. Before entering the bed, the nitrogen is heated using the 400 W in-line air process heater (Omega AHP-5052).

The ICFAR biomass “slug injector” is used to feed birch bark into the bubbling bed reactor (7). The birch bark is discharged into the bed, 0.15 m above the gas distributor through an inclined line (45°). As shown in Figure 3.1, a hopper filled with birch bark discharges through a pneumatically activated pinch valve. The pinch valve opens periodically (usually every 10 s) for short periods of time (0.7 s), allowing small amounts of birch bark to fall into a horizontal injector tube. During each cycle, the birch bark forms a slug, which is propelled into the reactor by intermittent pulses of nitrogen and a continuous stream of carrier gas (nitrogen). The continuous nitrogen flow prevents any solids settling in the injector tube. A solenoid valve is used to deliver this gas pulse. The pinch valve and the solenoid valve are controlled and synchronized with a programmable logic controller (PLC). The flow rates of the fluidization and carrier nitrogen are metered and controlled with two Omega mass flow meters.

As the birch bark is injected into the reactor, it mixes rapidly with the hot sand, ensuring fast pyrolysis conditions. The produced vapors exit the top of the reactor through a hot filter. The filter uses a stainless steel, 10 micron screen and a ceramic fiber insulation layer that retains all the solids in the reactor to avoid contamination of the produced bio-oil by char and elutriated sand. The product gases and vapors together with

the nitrogen gas flow into the condensing system where the bio-oil vapors are rapidly condensed using three condensers connected in series.

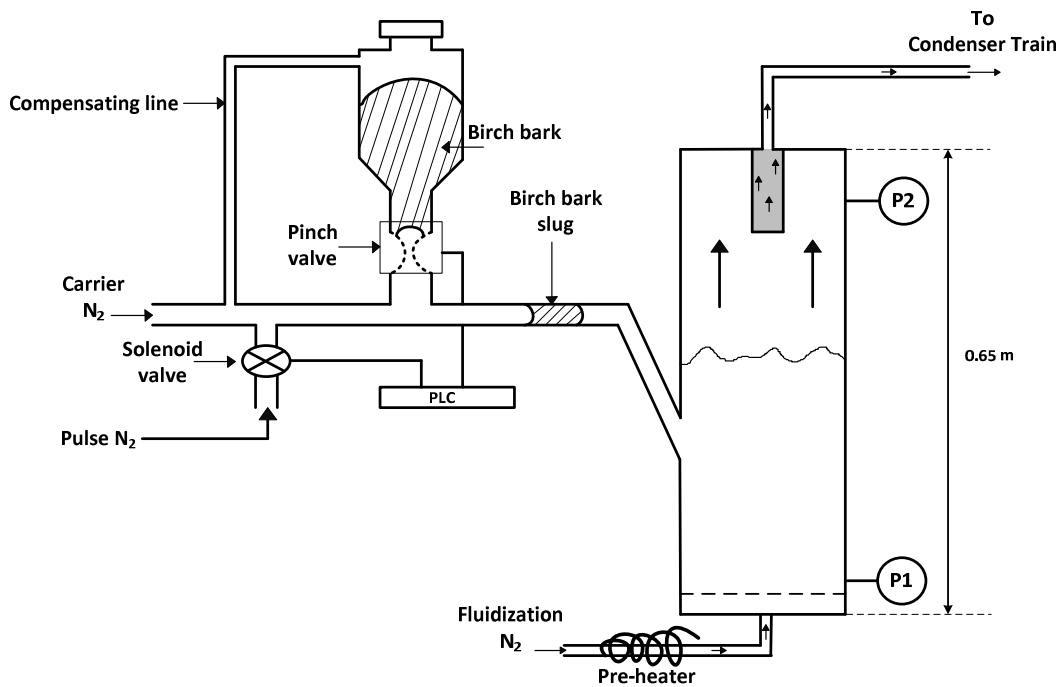


**Figure 3.1** Schematic of bubbling fluidized bed setup used for the pyrolysis of birch bark

### 3.2.3 Condensing system

The condensing system consists of two cyclonic condensers (condenser 1 and 3), an electrostatic precipitator-cum-condenser (C-ESP) and a cotton wool filter. As shown in Figure 3.2, the three condensers are connected in series such as the vapor/gas stream flows through condenser 1, then the C-ESP, condenser 3 and, finally, the cotton wool filter. In order to separate the water present in the bio-oil vapors, condenser 1 and C-ESP are maintained at higher temperatures, so that water is primarily condensed in condenser 3. The temperature of the stream leaving each condenser is constantly recorded using a K-type thermocouple placed at each condenser's outlet.

The cyclonic condensers (condenser 1 and 3) are made of a stainless steel pipe, 0.7 m long and 0.05 m in diameter. In the cyclonic condensers, the mixture of vapors and gases enters each condenser and is immediately directed to the condenser wall with a 90° elbow (shown in Figure 3.2). This nearly tangential entry forces the vapors and gases to spin, providing good agitation and heat transfer and driving the condensed liquid droplets to the wall through cyclonic action. The cyclonic condensers and the C-ESP can be independently weighed before and after each run to obtain an accurate liquid yield (9).

In all the experiments, condenser 1 is maintained at 80 °C to collect the vapors of the heavy components. Note that the high dilution of the vapors with the fluidization gas greatly depresses the dew point of the vapors. To maintain the desired temperature of the condenser 1, it is immersed in a temperature-controlled oil bath. The heat transfer fluid used in the bath is Duratherm G, which has a flash point of 223 °C. A high temperature cartridge heater, located at the bottom of the bath, maintains the bath fluid at the desired temperature. The temperature of the cartridge heater is controlled using a Watlow series C on-off temperature controller. To ensure a uniform temperature along the entire length of the condenser and also for good heat transfer from the walls of the condenser, nitrogen is bubbled at a very low flow rate in the bath fluid to provide sufficient mixing. The average temperature of the stream exiting the condenser 1 was around 105 °C.

The electrostatic precipitator-cum-condenser (C-ESP) is designed to accomplish dual functionalities: 1) To condense the vapors of the intermediate compounds by further cooling the stream leaving the first condenser; and 2) To collect the aerosols present in the product stream through electrostatic precipitation. As shown in Figure 3.2, the C-ESP consists of an electrostatic precipitator (ESP) enclosed in a hot box, which is heated by a

continuous flow of hot air from the bottom to the top of the box. A scaled-up version of the two-stage-ESP developed by Bedmutha et al. (10) is used in this study. The ESP is made of a stainless steel pipe, 0.6 m long and 0.06 m in diameter. Throughout the experimental study, the ESP is operated with an applied voltage of 14 kVDC. The temperature of the C-ESP can be varied by changing the hot air temperature entering the C-ESP enclosed chamber. An in-line air process heater (Omega AHP-7561), controlled using a Watlow series C on-off temperature controller, is used for the heating of the air. In the experiments conducted to optimize the fractional condensation train, the temperature of C-ESP was maintained at 30, 50 or 70 °C. While the C-ESP temperature was maintained at 30, 50 or 70 °C, the average temperature of the stream exiting the C-ESP was 38, 49 or 56 °C, respectively.

The third condenser, which has the objective to recover the majority of the water and the vapors of the lightest components, is placed in an ice water bath. The average temperature of the stream exiting the third condenser was below 15 °C. A cotton wool filter is connected downstream of the three condensers; it is weighed after each run to check the efficiency of collection in the condensing train. The non-condensable gases leaving the condensing system are vented.

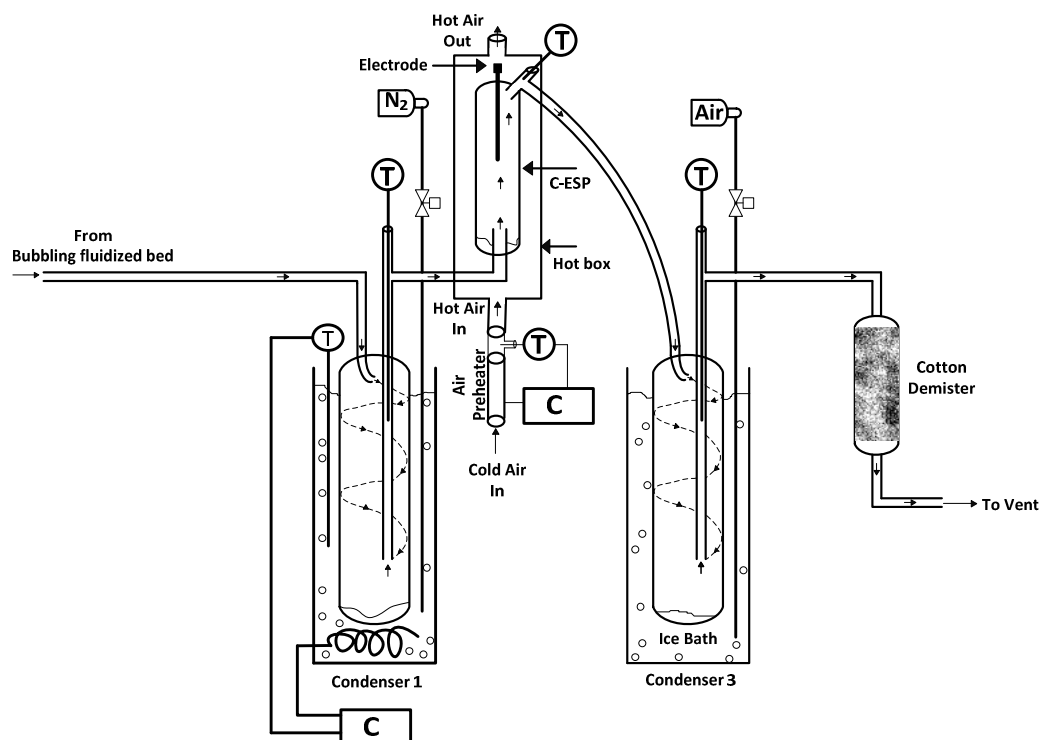


**Figure 3.2** Schematic of fractional condensing train used for the collection of birch bark bio-oil

### 3.2.4 Bio-oil production

In the course of optimization of the fractional condensation train, all the pyrolysis runs were performed at 550 °C and, during the optimization of the pyrolysis reaction temperature, experimental runs were carried out at reactor temperatures of 450, 500, 550 and 600 °C. The combined flow rate of nitrogen fluidization and carrier gases was adjusted from  $5.2 \times 10^{-4}$  to  $4.3 \times 10^{-4}$  kg/s when the bed temperature was changed from 450 to 600 °C, to keep the vapor residence time constant. Before each experiment, the temperature and the gas flow controllers were set to the desired value. All the experimental runs lasted between 25 and 35 minutes, for the pyrolysis of 200 grams of birch bark.

The total liquid bio-oil production was determined by weighing all the three condensers and the cotton wool filter before and after each run. Bio-oil samples recovered from the three condensers were analyzed individually.

### 3.2.5 Analysis of bio-oil fractions

**Water content:** The water content of the bio-oil samples was determined using a volumetric Karl Fischer titrator V20. Bio-oil recovered from the condenser 1 forms a solid wax at room temperature; the water content of this fraction was measured after liquefying the sample by heating.

**Higher heating value (HHV):** The HHV of each of the bio-oil samples from the three condensers was measured using an IKA C200 Oxygen Bomb Calorimeter following the ASTM D4809-00 standard method.

## 3.3 Experimental results and discussion

The experimental study proceeded through the following steps:

1. Selection of condenser temperatures to obtain a dry oil from the pyrolysis of birch bark;
2. Comparison with other fractional condensation trains;
3. Investigation of the impact of pyrolysis temperature on the dry bio-oil yield and characteristics; and
4. Comparison of the characteristics of dry bio-oil with commercial fuels.

**Table 3.1** Operating conditions used in all the experiments performed for the fractional condensation of bio-oil vapors produced from birch bark pyrolysis

<b>S. No</b>	<b>Pyrolysis Temperature (°C)</b>	<b>Condenser 1 Temperature (°C)</b>	<b>C-ESP Temperature (°C)</b>	<b>Condenser 3 Temperature (°C)</b>
1	550	80	30	0
2	550	80	50	0
3	550	80	70	0
4	450	80	70	0
5	500	80	70	0
6	600	80	70	0

### 3.3.1 Optimization of the fractional condensation train

Previous research publications on fast pyrolysis of biomass indicate that maximum liquid yields are obtained at pyrolysis temperatures ranging from 450 to 550 °C, with a short vapor residence time of 0.5 to 5 s (9, 11). During the optimization of the fractional condensation train, all the experiments were performed at a constant reactor temperature of 550 °C with a vapor residence time of 1.5 s.

In order to prevent condensation of water vapor present from the pyrolysis gas stream, the first condenser and C-ESP were operated at higher temperatures. Throughout the experimental study, the condenser 1 was maintained at 80 °C to collect the higher boiling point components present in the bio-oil vapor stream and the temperature of the C-ESP was varied from 30 to 70 °C. In all the experiments, the condenser 3 was maintained in an ice water bath for the collection of water and light organics.

### 3.3.1.1 Bio-oil distribution in different condensers

The bio-oil yields in the three condensers and the cotton filter at three operating temperatures (30, 50, and 70 °C) of the C-ESP are shown in Figure 3.3. Although the condenser 1 is operated at the same temperature in all the runs, Figure 3.3 shows slight variations in the bio-oil yield of condenser 1, which resulted from minor variations in the temperature of the first condenser. With the increase in C-ESP temperature, the bio-oil yield in the C-ESP decreased and the yield in condenser 3 increased. In all the cases, the amount of bio-oil captured by the cotton filter is less than 1% of the total, which indicates a near perfect functioning of the condenser train.

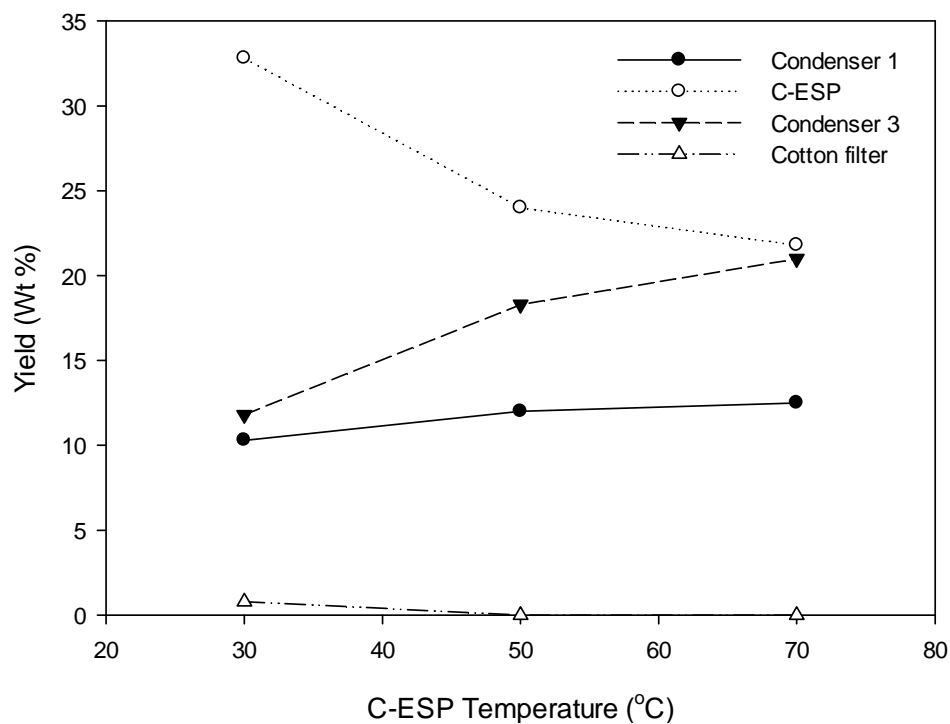


**Figure 3.3** Bio-oil yield in three condensers at different C-ESP temperatures

As condenser 1 and the C-ESP are intended to collect bio-oil with low water content, the liquids collected in condenser 1 and C-ESP were combined and hereafter referred as the “Oil fraction”. As the bio-oil captured by the cotton filter is very small, the bio-oil collected in the condenser 3 is hereafter referred as the “Water fraction”, and the very minor amount recovered in the cotton filter is assumed to have the same composition. Figure 3.4 shows that, as the C-ESP temperature is increased, the yield of the oil fraction decreased and the yield of the water fraction increased. Figure 3.4 also shows that the yield of the “raw bio-oil” is almost constant at 55% in all the three cases, showing very good reproducibility under the same operating condition of the bubbling bed reactor. The raw bio-oil is defined as the total bio-oil produced, and the yield of the raw bio-oil is the summation of the yields of bio-oil collected in the three condensers and the cotton filter.

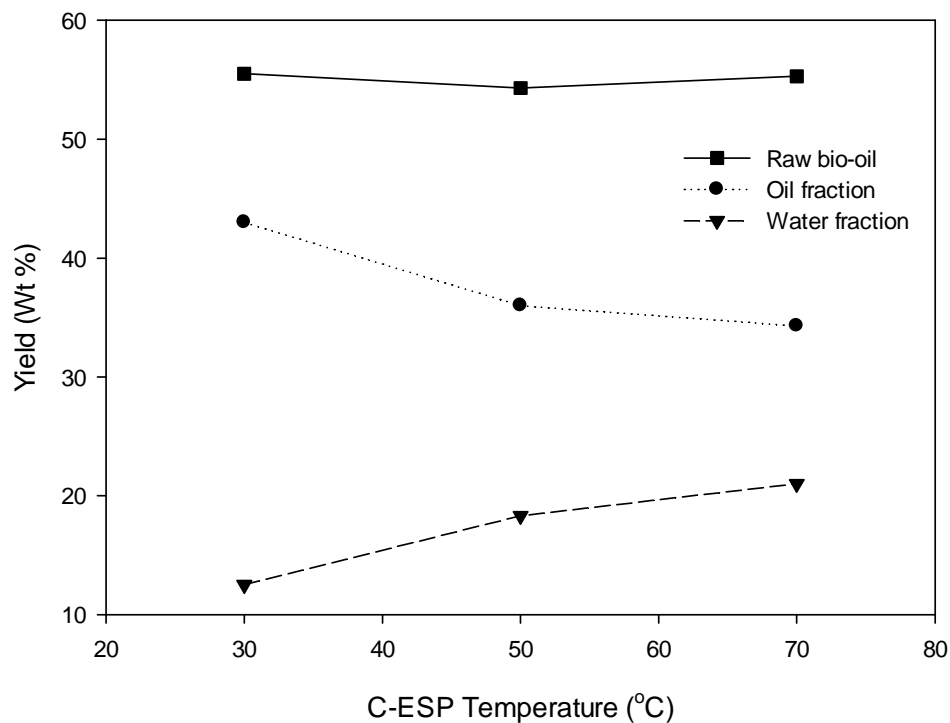


**Figure 3.4** Yields of oil fraction, water fraction, and raw bio-oil at different C-ESP temperatures

### 3.3.1.2 Water content of bio-oil fractions

Figure 3.5 shows that the water content of the oil fraction decreased with increasing C-ESP temperature, and reached a minimum of around 0.9% at the C-ESP temperature of 70 °C. The water content of the water fraction decreased from 75% to around 60% with the increase in C-ESP temperature. Considering both the water content and the yield of the oil fraction, the C-ESP operating temperature of 70 °C can be selected as the optimum for the recovery of dry bio-oil. The water content of the raw bio-oil is calculated by using the individual water content values of the bio-oils from the three condensers. The water content of the raw bio-oil is around 30% in all the three experiments.

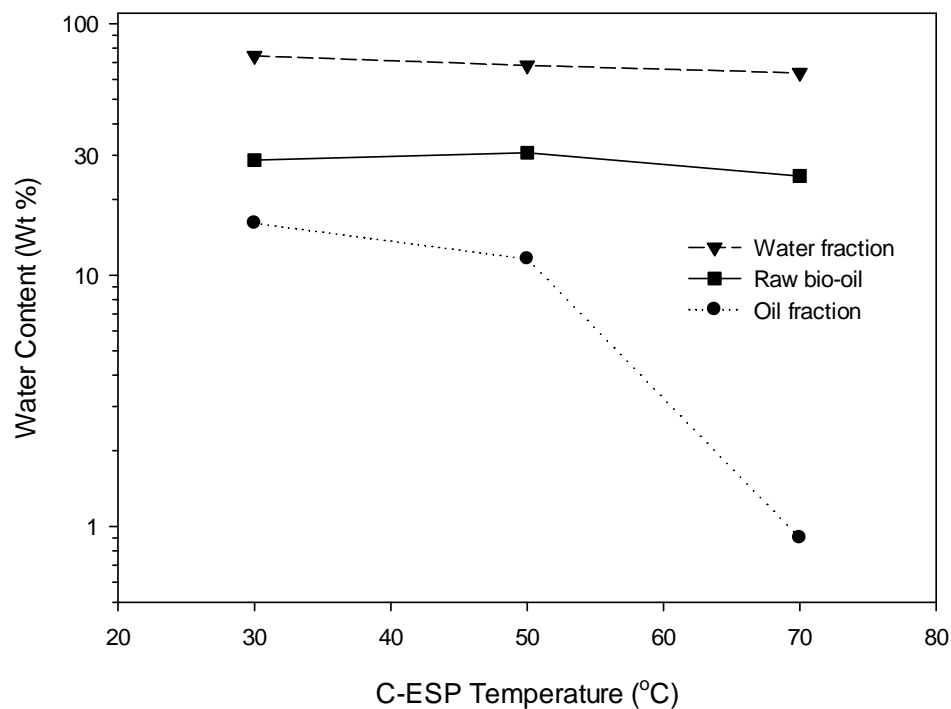


**Figure 3.5** Water content of oil fraction, water fraction, and raw bio-oil at different C-ESP temperatures

### 3.3.1.3 Variation in heating values of bio-oil fractions

Figure 3.6 shows the higher heating values of the oil fraction, water fraction and raw bio-oil at different C-ESP operating temperatures. The heating value of the raw bio-oil is calculated using the individual heating values of the bio-oils from the three condensers. Pollard et al. (6) reported that the heating value of their fractionated bio-oil with 6.6% water content was 24 MJ/Kg. The present study achieves significantly higher values since, at the optimum C-ESP temperature of 70 °C, the heating value of the oil fraction is around 31 MJ/Kg as compared to a heating value of 21 MJ/Kg for the raw bio-oil. As a result of removing the majority of the water from the raw bio-oil, the heating value of the dry bio-oil has increased by 48%. Figure 3.6 also shows that the heating

value of the water fraction increases with increasing C-ESP temperature, because it now contains light organics lost from the C-ESP.

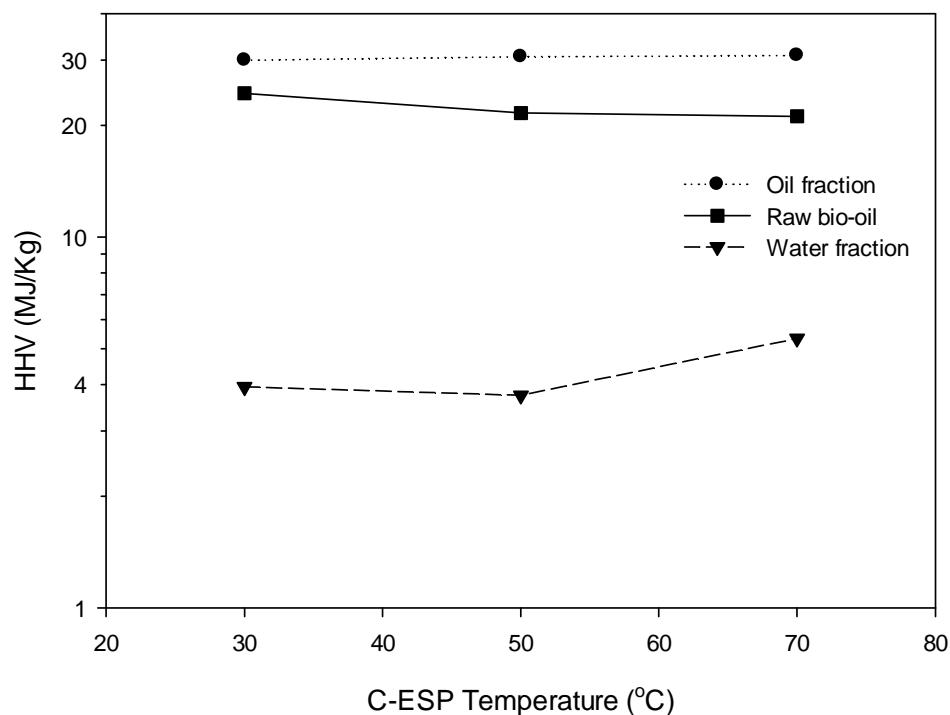


**Figure 3.6** Heating value of raw bio-oil, oil and water fractions at different C-ESP temperatures

#### 3.3.1.4 Energy recovered in oil fraction

Figure 3.6 indicates that there is loss of organics in the water fraction with increasing C-ESP temperature. It is essential to recover the maximum bio-oil energy in the oil fraction. Figure 3.7 shows the percentage of the raw bio-oil energy that is recovered in the oil fraction and the percentage that is lost in the water fraction, for the three different C-ESP temperatures. The bio-oil energy lost in the water fraction increases from around 3% to 10% with increasing C-ESP temperature. At the optimum C-ESP

temperature of 70 °C, the energy recovered in the oil fraction is, thus, 90% of the total bio-oil energy.

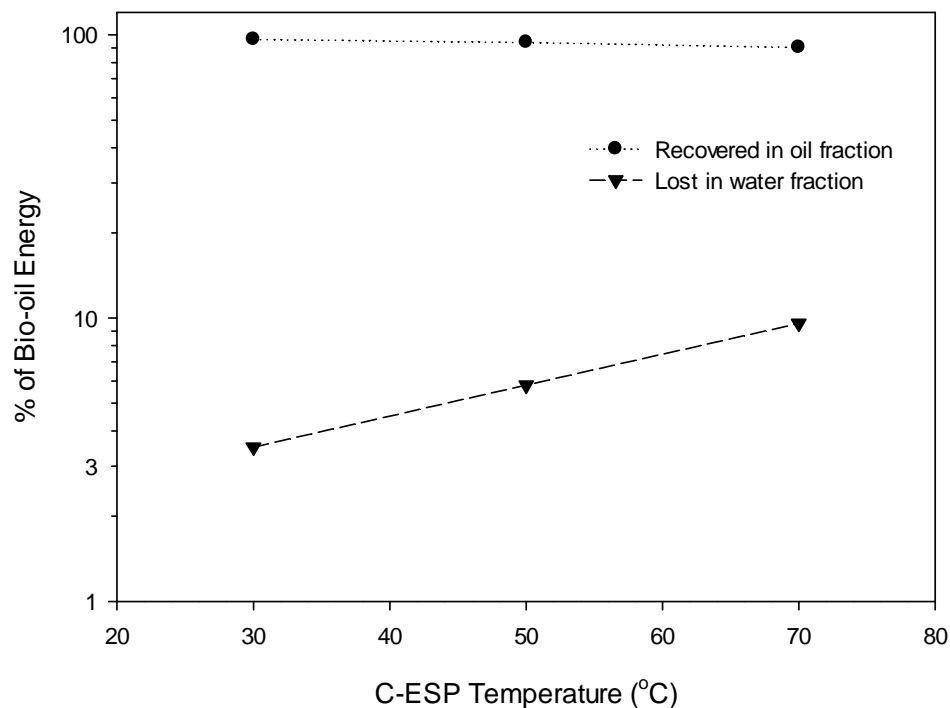


**Figure 3.7** Energy recovered in the oil and water fractions at different C-ESP temperatures

The water content, heating value and recovered bio-oil energy suggest that 70 °C should be selected as the optimum C-ESP operating temperature for the collection of dry bio-oil. At 70 °C, over 90% of the energy originally in the bio-oil is recovered in a dry oil fraction that contains less than 1% of water and has a high heating value.

### 3.3.2 Comparison with other fractional condensation trains

In this section, the performance of the fractional condensation train developed in this study is compared with the one developed by Pollard et al. (6). The key differences in

the physical properties of the bio-oil fractions obtained from the two fractional condensation systems, using similar bio-oil vapors, are shown in Table 3.2.

**Table 3.2** Comparison of physical properties of the bio-oil fractions obtained from two fractional condensation systems

	Pollard et al. (6)	This study
Minimum Water content (wt%)	6.6	0.9
Highest Heating value (MJ/kg)	24.2	31

The oil fraction obtained from our fractionating system has a much lower water content and a significantly higher heating value when compared to the oil fraction collected in the 1<sup>st</sup> stage of fractional condensation train by Pollard et al. (6). This improvement in the results is likely because of the initial optimization of the fractional condensation system carried out using bio-oil model compounds, described in Chapter 2. The differences in the design and the operating parameters of the two fractional condensation systems are listed in Table 3.3. An important difference is the cyclonic entry implemented in the condensers used in this study, which greatly enhances heat transfer to the condenser wall and gas mixing, as shown by the preliminary study with model compounds (described in Chapter 2).

**Table 3.3** Differences in design and operating parameters of the two fractional condensation systems

	Pollard et al. (6)	This study
Biomass	Red oak	Birch bark
Biomass injection flow rate (kg/hr)	8	0.4
N <sub>2</sub> flow rate (kg/hr)	12.75	1.76
Fluidization gas/biomass (dilution ratio, -)	1.6	4.4
Number of condensers/ESPs	5	3
Superficial velocity in condensers, ESPs (m/s)	-	Condensers - 0.6, ESP - 0.4
Residence time in condensers or ESPs (s)	1 – 10	Condensers - 1.2, ESP - 1.5
Heat transfer in condensers	Shell and tube, Laminar flow	Cyclonic entry, Laminar flow
Voltage in ESP (kVDC)	40	14

### 3.3.3 Optimization of pyrolysis reaction temperature

To investigate the effects of pyrolysis reaction temperature on the dry bio-oil yield and characteristics, experiments were performed at pyrolysis temperatures of 450, 500, 550 and 600 °C. During all the experiments, the vapor residence time was kept constant at 1.5 seconds. For all the experiments, the condenser 1, the C-ESP, and the condenser 3 were maintained at 80 °C, 70 °C, and in the ice water bath (0 °C), respectively.

#### 3.3.3.1 Bio-oil distribution in different condensers

Figure 3.8 shows that the yields of the raw bio-oil and the oil fraction follow the same trend. The pyrolysis carried out at 550 °C has the maximum yield for the raw bio-oil and the oil fraction, followed by 500, 450 and 600 °C. There is only a marginal difference in the yield of the oil fraction at pyrolysis temperature of 500 and 550 °C. The yield of the water fraction is almost constant at around 20% for all the reaction temperatures.

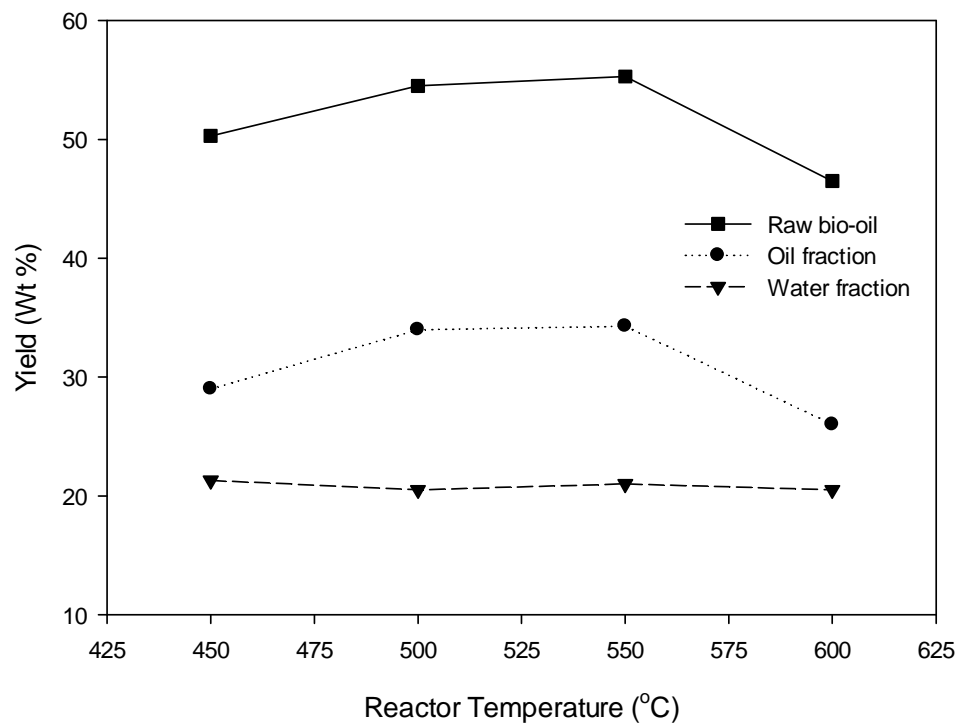


**Figure 3.8** Yields of raw bio-oil, oil and water fractions at different pyrolysis temperatures

### 3.3.3.2 Water content of bio-oil fractions

Figure 3.9 shows the variation in the water content of bio-oil fractions with the pyrolysis temperature. At all the pyrolysis temperatures, the water content of the raw bio-oil and the water fraction are around 25% and 60%, respectively. The water content of the oil fraction is less than 1% at all the pyrolysis temperatures. At 600 °C, there is a small decrease in the water content of the oil fraction from 0.9 to 0.7%.

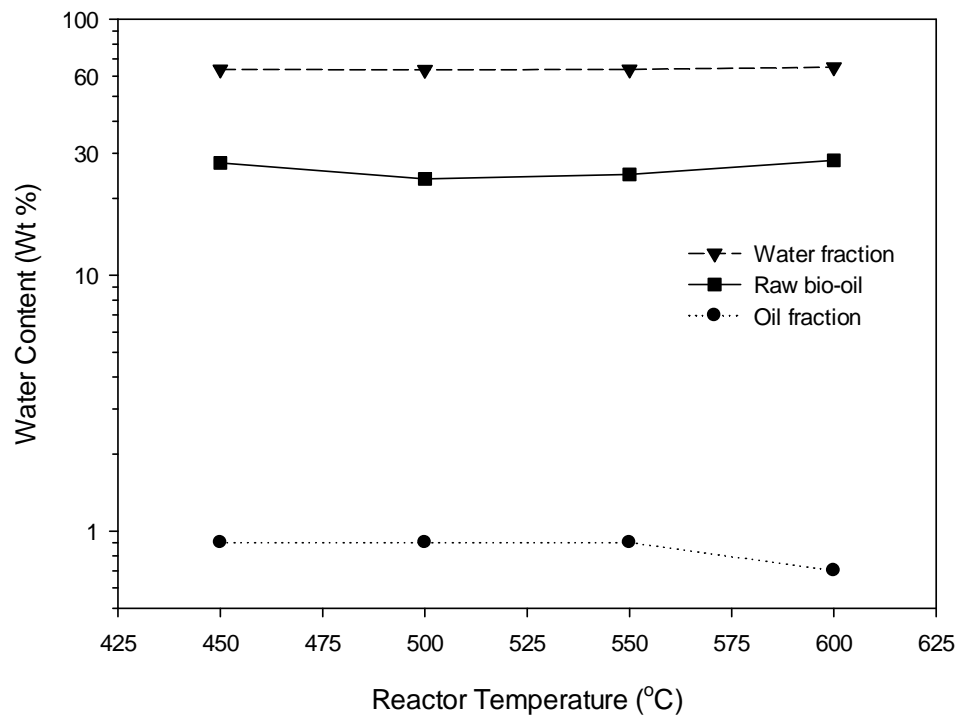


**Figure 3.9** Water content of raw bio-oil, oil and water fractions at different pyrolysis temperatures

### 3.3.3.3 Variation in heating value of bio-oil fractions

Figure 3.10 shows that there is no change in the heating value of the raw bio-oil and the oil fraction with the increase in the pyrolysis temperature. The heating values of the raw bio-oil and the oil fraction are around 21 and 31 MJ/Kg, respectively. With the increase in the pyrolysis temperature, there is a marginal decrease in the heating value of the water fraction.

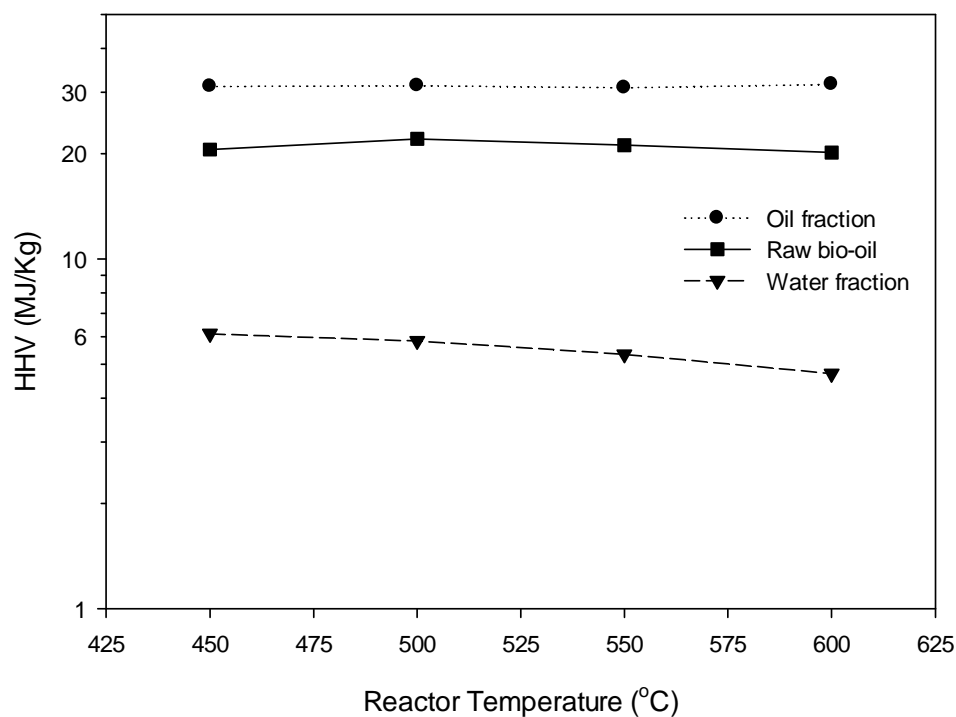


**Figure 3.10** Heating value of raw bio-oil, oil and water fractions at different pyrolysis temperatures

#### 3.3.3.4 Energy recovered in oil fraction

As mentioned earlier, most of the energy contained in the original bio-oil is recovered in the oil fraction. Figure 3.11 shows that nearly 90% of the raw bio-oil energy is recovered in the oil fraction at all the pyrolysis temperatures.

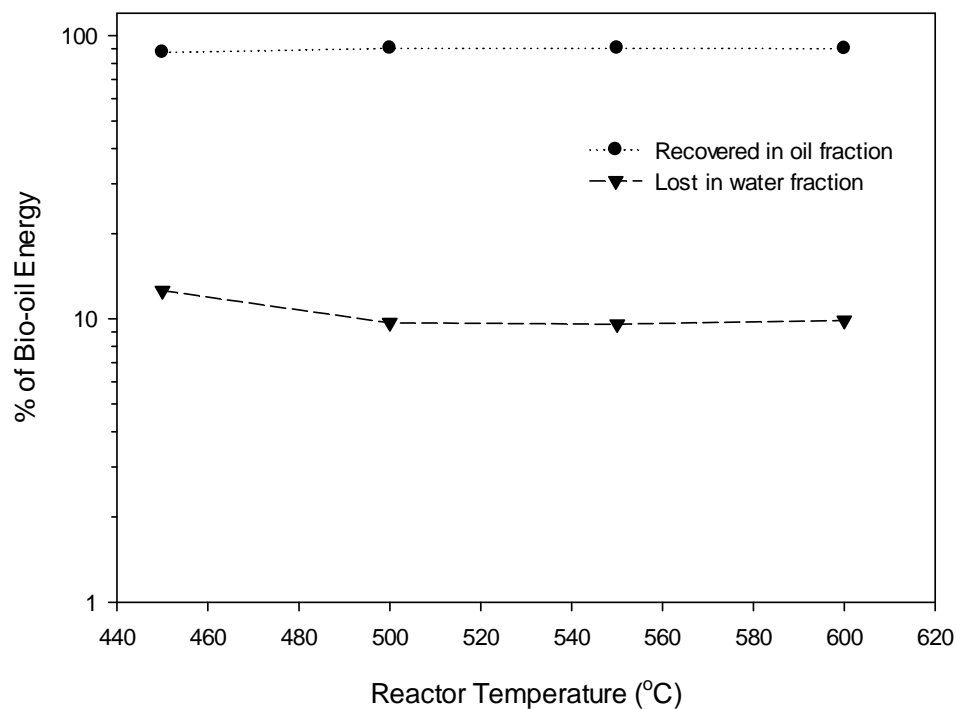


**Figure 3.11** Energy recovered in oil fraction at different pyrolysis temperatures

There is no significant change in the oil fraction water content and heating value when the pyrolysis temperature is varied from 450 to 600 °C. The best pyrolysis temperatures are 500 and 550 °C, for which the yield and quality of the dry oil fraction are maximized, as well as the energy recovery in the dry oil.

### 3.3.4 Fractioned birch bark bio-oil as a bio-fuel, comparison with traditional fuels

From Figure 3.12, it is apparent that the heating value of the dry bio-oil is slightly higher than that of ethanol. Currently, ethanol is being used as biofuel additive for gasoline.

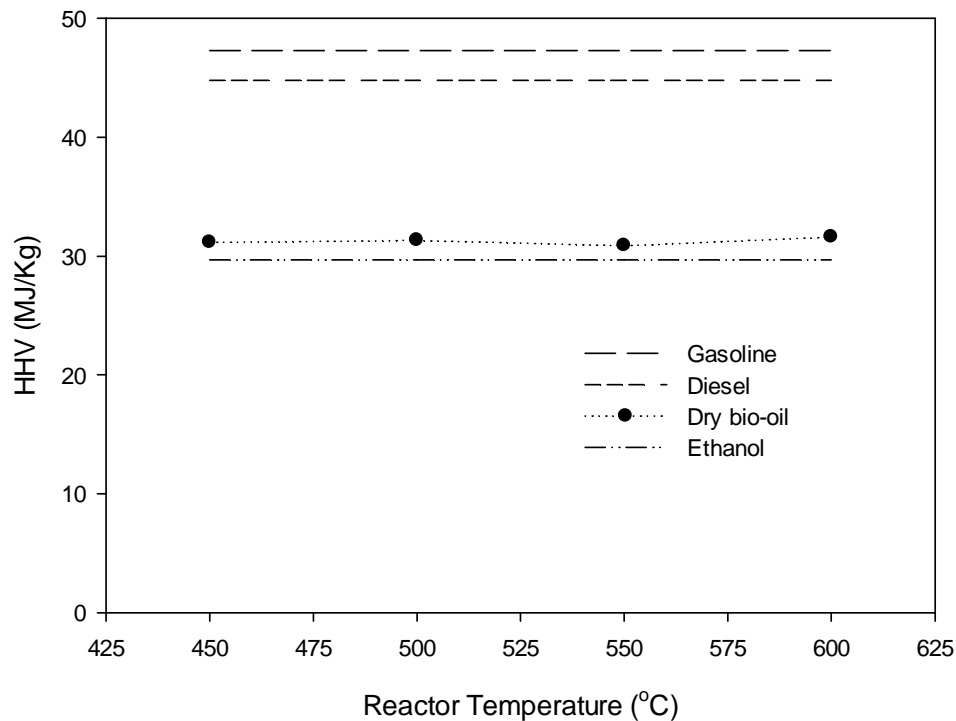


**Figure 3.12** Heating value of dry bio-oil and other commercial fuels

### 3.4 Conclusions

Birch bark was pyrolyzed in a bubbling bed reactor and the resulting bio-oil vapors were fractionated with a series of three temperature-controlled condensers consisting of an electrostatic precipitator-cum-condenser (C-ESP) between two cyclonic condensers. The temperatures of the condensers were optimized to obtain a nearly water free (less than 1 wt%) dry bio-oil in the first two condensers and a water-rich product in the third condenser.

Pyrolysis reactor temperatures of 500 and 550 °C maximized the yield of dry bio-oil. About 90% of the energy originally present in the raw bio-oil was recovered in the

dry bio-oil. The fact that this dry bio-oil fraction has a HHV slightly better than the ethanol makes fractional condensation a promising process to produce high quality fuels.

### 3.5 Acknowledgments

The authors would like to acknowledge funding from the Lignoworks network ([www.lignoworks.ca](http://www.lignoworks.ca)). They would also like to acknowledge help from Rob Taylor, and Caitlin Marshall.

### 3.6 References

- (1) Bridgwater AV. Renewable fuels and chemicals by thermal processing of biomass. *Chem Eng J* 2003 3/15;91(2–3):87-102.
- (2) Oasmaa A, Czernik S. Fuel oil quality of biomass pyrolysis oils - state of the art for the end users. *Energy and Fuels* 1999;13(4):914-921.
- (3) Chen T, Deng C, Liu R. Effect of selective condensation on the characterization of bio-oil from pine sawdust fast pyrolysis using a fluidized-bed reactor. *Energy and Fuels* 2010;24(12):6616-6623.
- (4) Jendoubi N, Broust F, Commandre JM, Mauviel G, Sardin M, Lédé J. Inorganics distribution in bio oils and char produced by biomass fast pyrolysis: The key role of aerosols. *J Anal Appl Pyrolysis* 2011;92(1):59-67.
- (5) Westerhof RJM, Brilman DWF, Garcia-Perez M, Wang Z, Oudenhoven SRG, Van Swaaij WPM, et al. Fractional condensation of biomass pyrolysis vapors. *Energy and Fuels* 2011;25(4):1817-1829.
- (6) Pollard AS, Rover MR, Brown RC. Characterization of bio-oil recovered as stage fractions with unique chemical and physical properties. *J Anal Appl Pyrolysis* 2012;93:129-138.

- (7) Berruti FM, Ferrante L, Berruti F, Briens C. Optimization of an intermittent slug injection system for sawdust biomass pyrolysis. *International Journal of Chemical Reactor Engineering* 2009;7.
- (8) Palmisano P, Berruti FM, Lago V, Berruti F, Briens C. Lignin Pyrolysis in a Fluidized Bed Reactor. *Tcbiomass*; 2011.
- (9) Xu R, Ferrante L, Briens C, Berruti F. Flash pyrolysis of grape residues into biofuel in a bubbling fluid bed. *J Anal Appl Pyrolysis* 2009;86(1):58-65.
- (10) Bedmutha RJ, Ferrante L, Briens C, Berruti F, Inculet I. Single and two-stage electrostatic demisters for biomass pyrolysis application. *Chemical Engineering and Processing: Process Intensification* 2009;48(6):1112-1120.
- (11) Bridgwater AV, Meier D, Radlein D. An overview of fast pyrolysis of biomass. *Org Geochem* 1999 26 November 1998 through 27 November 1998;30(12):1479-1493.

## **4 Chapter 4: Lignin pyrolysis and fractional condensation of its bio-oil vapors**

### **4.1 Introduction**

Lignin is the second most abundant biomass component after cellulose and constitutes up to 40% of the dry mass of wood. Also, it is the largest source of aromatics in nature. Kraft pulping is the predominant chemical process used by the pulp and paper industry to extract cellulose from wood by separating the lignin. Therefore, a by-product of Kraft pulping is the lignin-rich black liquor that is usually burned in recovery boilers. In some plants, recovery boiler capacity is limited and lignin may be extracted from some of the black liquor to debottleneck the plant. The lignin is then usually treated as a waste product and mainly used as a low grade fuel for energy recovery. Because of its availability in large quantities and its large aromaticity, Kraft lignin is considered as a valuable biomass source for the potential production of renewable fuels and chemicals (1, 2).

In the last 30 years, there have been major developments in the fast pyrolysis technology, which converts solid biomass to energy-dense, transportable liquid, together with solid co-products (bio-char) and non-condensable hydrocarbon gases. Fast pyrolysis can produce high liquid yields of up to 75%, based on the type of biomass, through rapid thermal decomposition of lignocellulosic biomass in the absence of oxygen. However, fast pyrolysis of lignin is not widely investigated because of the difficulties faced during the continuous feeding and processing of lignin in fluidized bed reactors. Due to its low melting point (between 150 and 200 °C), lignin is usually found to melt even before entering the reactor, causing blockage of the feeding systems. Other problem encountered

during lignin pyrolysis is the slow reactivity, resulting in the formation of a liquid phase in the reactors leading to the bed agglomeration and subsequent defluidization. The liquid yield resulting from the condensable vapors from the lignin pyrolysis is quite low and is reported in the range of 20 to 37 wt% (3-5).

Fast pyrolysis liquid, also called bio-oil, has tremendous potential as a fuel oil substitute. The heating value of raw bio-oils is around 17 MJ/kg, which is equivalent to approximately 40% of the heating value of diesel. The relatively low heating value of the bio-oil is due to its high water concentration (typically in the range between 15 and 30 wt%) and high oxygen content (35 – 40%). Bio-oils also have other undesirable properties for fuel application, such as low thermal stability, high corrosiveness and high acidity. The upgrading of bio-oils is crucial to convert bio-oils into stable liquid fuels (6, 7).

The heating value, corrosiveness and the phase stability of the bio-oils can be greatly improved by decreasing the water content of the bio-oils. Lately, researchers around the world have been extensively investigating the fractional condensation method for the separation of the constituents of the bio-oil (8-11). In the fractional condensation process, the bio-oil vapor stream from the fast pyrolysis reactor is passed through a series of condensers maintained at different, gradually decreasing temperatures to allow the collection of liquid fractions of different physical and chemical properties in each condenser.

In Chapter 3, we used a series of three temperature controlled condensers to collect dry bio-oil, i.e. with very low water content, from the pyrolysis of birch bark. The

condenser train consisted of an electrostatic precipitator-cum-condenser (C-ESP) installed between two cyclonic condensers.

The objective of the present work is to obtain dry bio-oil from the pyrolysis of Kraft lignin in order to generate a high value and stable feedstock for the possible production of phenols and fuel products. Kraft lignin is pyrolyzed in a modified bubbling fluidized bed equipped with an internal mechanical stirrer, and the resulting bio-oil vapors are fractionated to obtain a dry bio-oil. The fractionation of lignin bio-oil vapors is performed using the same condenser train that was successfully used to produce dry bio-oil from the pyrolysis of birch bark, described in Chapter 3. The effect of reactor temperature on the yield and characteristics of dry bio-oil will also be studied.

## **4.2 Materials and methods**

### **4.2.1 Materials**

Kraft lignin was used as the feedstock. The Kraft lignin was pyrolyzed without any pre-treatment. The bulk density and the higher heating value of Kraft lignin were  $330 \text{ kg/m}^3$  and  $26 \text{ MJ/kg}$ , respectively.

Inert silica sand with a Sauter-mean diameter of  $180 \text{ }\mu\text{m}$  was used as the bed material in the bubbling fluidized bed. The bed mass was 800 grams.

Nitrogen was used as the inert fluidization gas. Nitrogen was also the gas used in the pulsating feeder used to introduce the Kraft lignin into the bubbling bed.

#### 4.2.2 Bubbling fluidized bed setup

The fluidized bed reactor is made of Inconel 600, 0.075 m in diameter, with a 0.65 m long cylindrical section (5). The reactor is heated by three irradiative electric heaters, covering the dense sand bed and the freeboard sections. The heaters are independently controlled using Watlow PID digital controllers, to set a constant temperature profile along the axis of the reactor. The temperature feedback for the Watlow controllers is provided through type K thermocouples placed within the bed at the same height as the heaters. The reactor is equipped with an internal stirrer, made with three blades of Inconel, to break the agglomerates formed by char and sand during the pyrolysis of lignin (4). The nitrogen fluidization gas enters the bed through a perforated distributed plate located at the bottom of the reactor. Before entering the bed, the nitrogen is heated using a 400 W in-line air process heater (Omega AHP-5052).

The ICFAR biomass “slug injector” is used to feed lignin into the bubbling bed reactor (12). As shown in Figure 4.1, a hopper filled with lignin discharges through a pneumatically activated pinch valve. The pinch valve opens periodically (usually every 10 s), for short periods of time (0.4 s), allowing small amounts of lignin to fall into a horizontal injector tube. During each cycle, the lignin forms a slug, which is propelled into the reactor by intermittent pulses of nitrogen and a continuous stream of carrier gas (nitrogen). The continuous nitrogen prevents any solids settling in the injector tube. A solenoid valve is used to deliver this gas pulse. The pinch valve and the solenoid valve are controlled and synchronized with a programmable logic controller (PLC). The flow rates of the fluidization and carrier nitrogen are metered and controlled with two Omega mass flow meters. The lignin is injected into the bed, 0.15 m above the gas distributor

through a cooled and inclined line (45°). The feeding line is cooled using ice-water-cooled jacket in order to avoid the blockage of the feeding line due to premature melting of the lignin before entering the reactor (4).

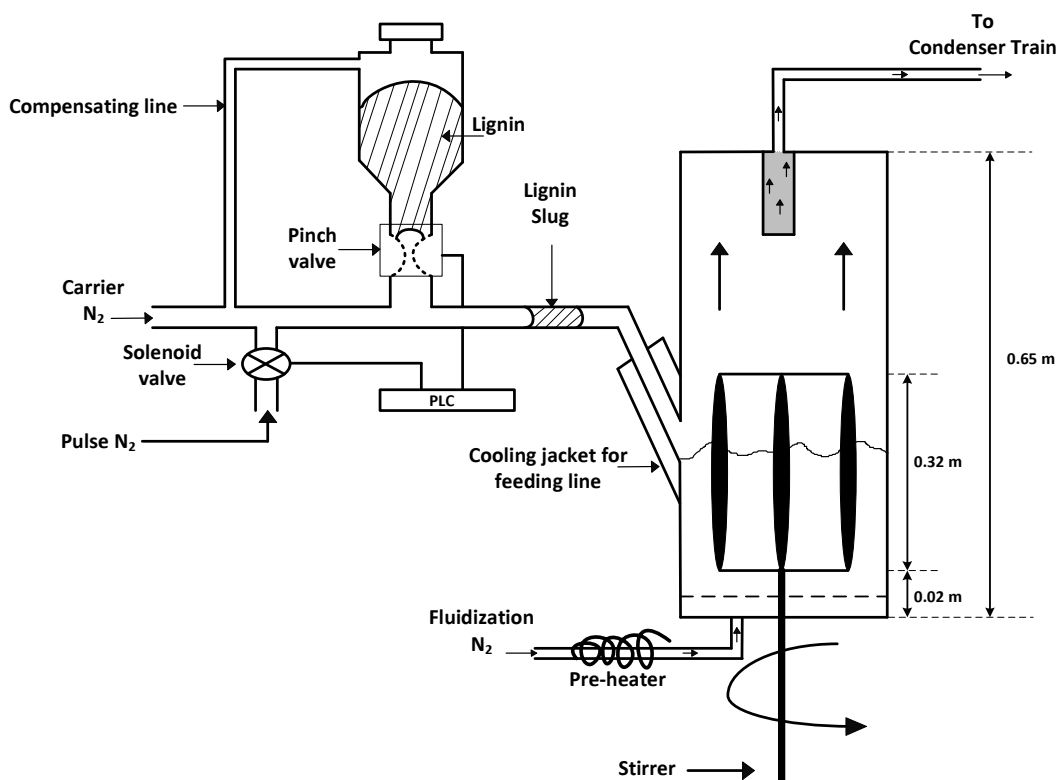


**Figure 4.1** Schematic of bubbling fluidized bed setup used for the pyrolysis of lignin

Once the lignin is injected into the reactor, the mechanical stirrer increases the mixing between the hot sand and the liquid lignin and prevents the formation of agglomerates, consequently ensuring better conditions for the fast pyrolysis. The mechanical stirrer used in the fluidized bed reactor is shown in Figure 4.2. During all the experiments, the mechanical stirrer is operated at a frequency of 40 rpm. The agglomeration formed in the fluidized bed reactor in the absence of mechanical stirrer is shown in Figure 4.3. The produced vapors exit the top of the reactor through a hot filter. The filter uses a stainless steel, 40 micron screen and a ceramic fiber insulation layer that

retains all the solids in the reactor to avoid contamination of the produced bio-oil by char or elutriated sand. The product gases and vapors together with the nitrogen gas flow into the condensing system where the bio-oil vapors are rapidly condensed using three condensers connected in series.



**Figure 4.2** Mechanical stirrer used in the fluidized bed



**Figure 4.3** Agglomeration in the fluidized bed in the absence of mechanical stirrer

#### 4.2.3 Condensing system

The condensing system consists of two cyclonic condensers (condenser 1, 3), an electrostatic precipitator-cum-condenser (C-ESP) and a cotton wool filter. As shown in

Figure 4.4, the three condensers are connected in series and the vapor/gas stream flows through condenser 1, then the C-ESP, condenser 3 and, finally, the cotton wool filter. In order to separate the water present in the bio-oil vapors, condenser 1 and C-ESP are maintained at higher temperatures so that water is primarily condensed in condenser 3. The temperature of the stream leaving each condenser is constantly recorded using a K-type thermocouple placed at each condenser's outlet.

The cyclonic condensers (condenser 1 and 3) are made of a stainless steel pipe, 0.7 m long and 0.05 m in diameter. In the cyclonic condensers, the mixture of vapors and gases enters each condenser and is immediately directed to the condenser wall with a 90° elbow (shown in Figure 4.4). This nearly tangential entry forces the vapors and gases to spin, providing good agitation and heat transfer and driving the condensed liquid droplets to the wall through cyclonic action. The cyclonic condensers and the C-ESP can be independently weighed before and after each run to obtain an accurate liquid yield (13).

In all the experiments, condenser 1 is maintained at 80 °C to condense the vapors of the heavy components. Note that the high dilution of the vapors with fluidization gas greatly depressed the dew point of the vapors. To maintain condenser 1 at the desired temperature, it is immersed in a temperature-controlled oil bath. The heat transfer fluid used in the bath is Duratherm G, which has a flash point of 223 °C. A high temperature cartridge heater, located at the bottom of the bath, maintains the bath fluid at the desired temperature. The temperature of the cartridge heater is controlled using a Watlow series C on-off temperature controller. To ensure a uniform temperature along the entire length of the condenser and also for good heat transfer from the walls of the condenser, nitrogen

is bubbled at a very low flow rate in the bath fluid to provide sufficient mixing. The average temperature of the stream exiting the condenser 1 was around 100 °C.

The electrostatic precipitator-cum-condenser (C-ESP) is designed to accomplish dual functionalities: 1) To condense the vapors of the intermediate compounds by further cooling the stream leaving the first condenser; 2) To collect the aerosols present in the product stream through electrostatic precipitation. As shown in Figure 4.4, C-ESP consists of an electrostatic precipitator (ESP) enclosed in a hot air box, which is heated by a continuous flow of hot air from the bottom to the top of the box. A scaled up version of the two-stage-ESP developed by Bedmutha et al. (14) is used in this study. The ESP is made of stainless steel pipe, 0.6 m long and 0.06 m in diameter. Throughout the experimental study, the ESP is operated with an applied voltage of 14 kVDC. The temperature of the C-ESP can be varied by changing the hot air temperature entering the C-ESP enclosed chamber. An in-line air process heater (Omega AHP-7561), controlled using a Watlow series C on-off temperature controller, is used for air heating. In the experiments conducted to optimize the fractional condensation train, the temperature of the C-ESP was maintained at 40, 50 or 70 °C. While the C-ESP was maintained at 40, 50 or 70 °C, the average temperature of the stream exiting the C-ESP was 41, 46 or 56 °C, respectively.

The third condenser, which has the objective to recover all the water and the light components vapors, is placed in an ice water bath. The average temperature of the stream exiting the third condenser was below 10 °C. A cotton wool filter is connected downstream of the three condensers; it is weighed after each run to check the efficiency

of collection in the condensing train. The non-condensable gases leaving the condensing system are vented.

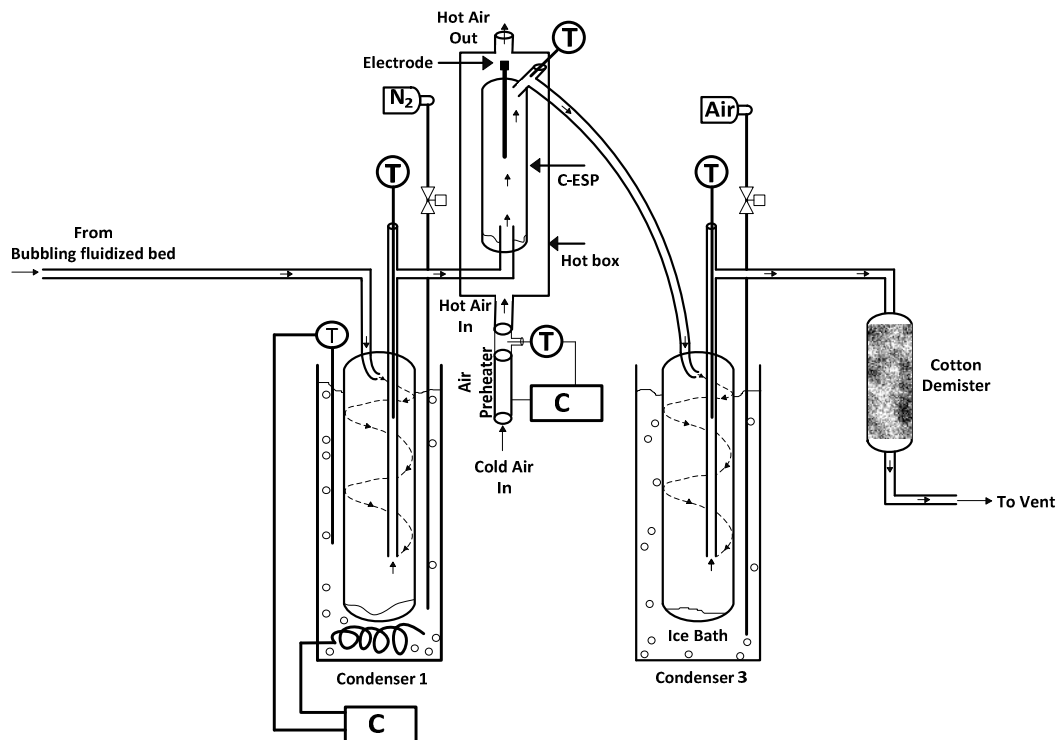


**Figure 4.4** Schematic of fractional condensing train used for the collection of lignin bio-oil

#### 4.2.4 Bio-oil production

During the optimization of fractional condensation train, all the pyrolysis runs were performed at 550 °C and during the optimization of pyrolysis reaction temperature, experimental runs were carried out at reactor temperatures of 450, 500, 550 and 600 °C. The combined flow rate of fluidization and carrier gases was adjusted from  $5.2 \times 10^{-4}$  to  $4.3 \times 10^{-4}$  kg/s when the bed temperature was changed from 450 to 600 °C, to keep the vapor residence time constant at 1.5 s. Before each experiment, the temperature and the

gas flow controllers were set to the desired value. The duration of the experimental runs ranged from 20 to 30 minutes, for the pyrolysis of 200 grams of lignin.

The total liquid bio-oil production was calculated by weighing all the three condensers and the cotton wool filter before and after each run. Bio-oil samples collected from the three condensers were analyzed individually.

#### 4.2.5 Analysis of bio-oil fractions

**Water content:** The water content of the bio-oil samples was measured using a volumetric Karl Fischer titrator V20. Bio-oil condensed in the condenser 1 forms a solid wax at room temperature; the water content of this fraction was measured after liquefying the sample by heating.

**Higher heating value (HHV):** The HHV of bio-oil samples from the three condensers was determined using an IKA C200 Oxygen Bomb Calorimeter following the ASTM D4809-00 standard method.

**Chemical composition of bio-oil:** The chemical composition of some of the bio-oil samples was determined by a Shimadzu GC-MS/FID system. For the GC-MS/FID analysis, the samples were prepared as a mixture of 50 $\mu$ L of bio-oil, 50  $\mu$ L of internal standard solution (1-dodecanol, 10 g/L) and 1000  $\mu$ L of methanol . The sample injection parameters, column and system operating conditions, and peak integration parameters are shown in the Table 4.1.

**Table 4.1** Details of GC-MS/FID system

GC-MS/FID	Shimadzu GCMS-QP2010 plus, equipped with auto sampler/injector AOC-20i+s
Column	RTX-1701, i.d., 0.25 mm, length 30 m, film thickness 0.25 $\mu\text{m}$ , max. temperature 280 $^{\circ}\text{C}$
Sample Injection	Injection volume 1 $\mu\text{L}$ , carrier gas He, split ratio 20:1, injection temperature 280 $^{\circ}\text{C}$ , column flow 0.75 mL/min, constant linear velocity control
Column Oven Temperature Program	Initial temperature 45 $^{\circ}\text{C}$ (hold 3 min), increasing to 220 $^{\circ}\text{C}$ at 5 $^{\circ}\text{C}/\text{min}$ , then to 280 $^{\circ}\text{C}$ at 30 $^{\circ}\text{C}/\text{min}$ , and holding for 3 min.
MS detector settings	Ion source temperature 200 $^{\circ}\text{C}$ , interface temperature 280 $^{\circ}\text{C}$ , solvent cut time 2.5 min
FID detector settings	Temperature 300 $^{\circ}\text{C}$ , makeup flow 30 mL/min, $\text{H}_2$ flow 35 mL/min, air flow 350 mL/min
Peak integration parameters	Width: 3 s, Slope: 800 $\mu\text{L}/\text{min}$ , Drift: 0 $\mu\text{L}/\text{min}$ , T.DBL: 100 min, Min. Area/Height: 500 counts

### 4.3 Experimental results and discussion

The study is carried out in the following steps:

1. Selection of condenser temperatures to collect a dry oil from the pyrolysis of lignin;
2. Study of the impact of pyrolysis temperature on the dry bio-oil yield and characteristics; and
3. Comparison of the heating value of dry bio-oil with commercial fuels

**Table 4.2** Operating conditions used in all the experiments performed for the fractional condensation of bio-oil vapors produced from lignin pyrolysis

<b>S. No</b>	<b>Pyrolysis Temperature (°C)</b>	<b>Condenser 1 Temperature (°C)</b>	<b>C-ESP Temperature (°C)</b>	<b>Condenser 3 Temperature (°C)</b>
1	550	80	40	0
2	550	80	50	0
3	550	80	70	0
4	450	80	70	0
5	500	80	70	0
6	600	80	70	0

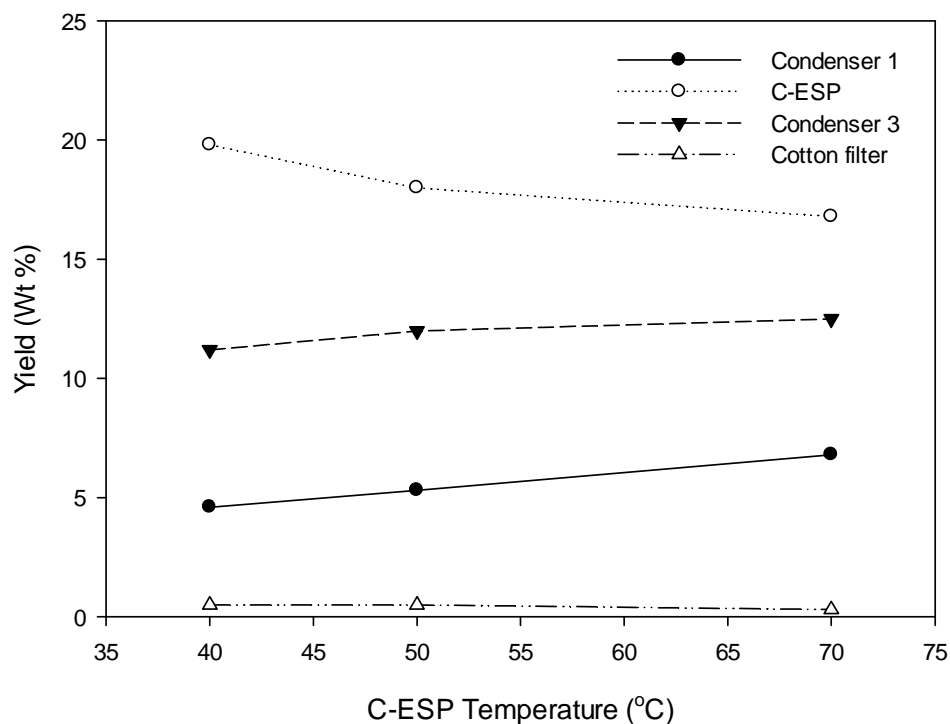
#### 4.3.1 Optimization of fractional condensation train

From the previous published data on fast pyrolysis of biomass, it is well known that maximum bio-oil yields are obtained at pyrolysis temperatures ranging from 450 to 550 °C, with a short vapor residence time of 0.5 to 5 s (13, 15). During the selection of condenser temperatures, all the experiments were performed at a reactor temperature of 550 °C with a vapor residence time of 1.5 s.

In order to prevent condensation of the water vapor present in the pyrolysis gas stream, the first condenser and C-ESP were maintained at high temperatures. All through the experimental study, the first condenser was operated at 80 °C to collect the higher boiling point components present in the bio-oil vapor stream and the temperature of the C-ESP was increased from 40 to 70 °C. In all the experiments, the condenser 3 was immersed in an ice water bath for the condensation of water and light organics.

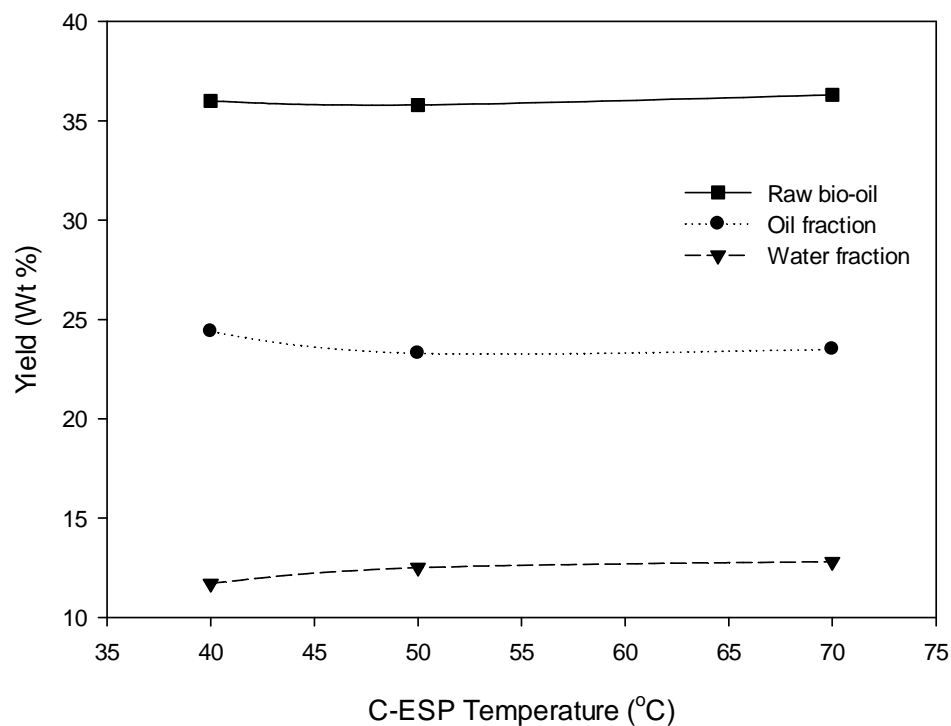
#### 4.3.1.1 Bio-oil distribution in different condensers

Figure 4.5 shows the variation of the bio-oil yields in the three condensers and the cotton filter with the operating temperature of the C-ESP. Even though the condenser 1 is operated at the same temperature in all the three experiments, Figure 3 shows a slight increase in the bio-oil yield of condenser 1, which is caused by minor changes in the temperature of the first condenser. With the increase in C-ESP temperature from 40 to 70 °C, the bio-oil yield of the C-ESP decreased and the yield of condenser 3 increased. In all the three experiments, the bio-oil yield of the cotton filter is less than 1%, which indicates efficient functioning of the condenser train.



**Figure 4.5** Bio-oil yield in three condensers for different C-ESP temperatures

As the first condenser and the C-ESP are expected to collect bio-oil with low water content, the bio-oils recovered in condenser 1 and C-ESP are combined and hereafter referred as the “oil fraction”. As the bio-oil captured by the cotton filter is very small, the bio-oil recovered in the condenser 3 is hereafter referred as the “water fraction”, and the very minor amount recovered in the cotton filter is assumed to have the same composition. Figure 4.6 shows that as the C-ESP temperature is increased, the yield of the oil fraction is slightly decreased and the yield of the water fraction is slightly increased. The raw bio-oil is defined as the total bio-oil produced, and the yield of the raw bio-oil is the summation of the yields of bio-oil collected in the three condensers and the cotton filter. Figure 4.6 also shows that the yield of the “raw bio-oil” is around 36 wt% in all the three experiments, showing very good reproducibility under the same operating condition of the bubbling bed reactor.



**Figure 4.6** Yields of oil fraction, water fraction, and raw bio-oil at different C-ESP temperatures

#### 4.3.1.2 Water content of bio-oil fractions

The water content of the raw bio-oil is calculated by using the individual water content values of the bio-oils from the three condensers. Figure 4.7 shows that the water content of the raw bio-oil is around 30% in all the three experiments. As the C-ESP temperature is increased from 40 to 70 °C, the water content of the oil fraction decreases from 1.9 to 0.9%, while the water content of the water fraction slightly decreases from 89% to 87%. Considering both the water content and the yield of the oil fraction, the C-ESP operating temperature of 70 °C can be selected as optimum for the collection of dry bio-oil.

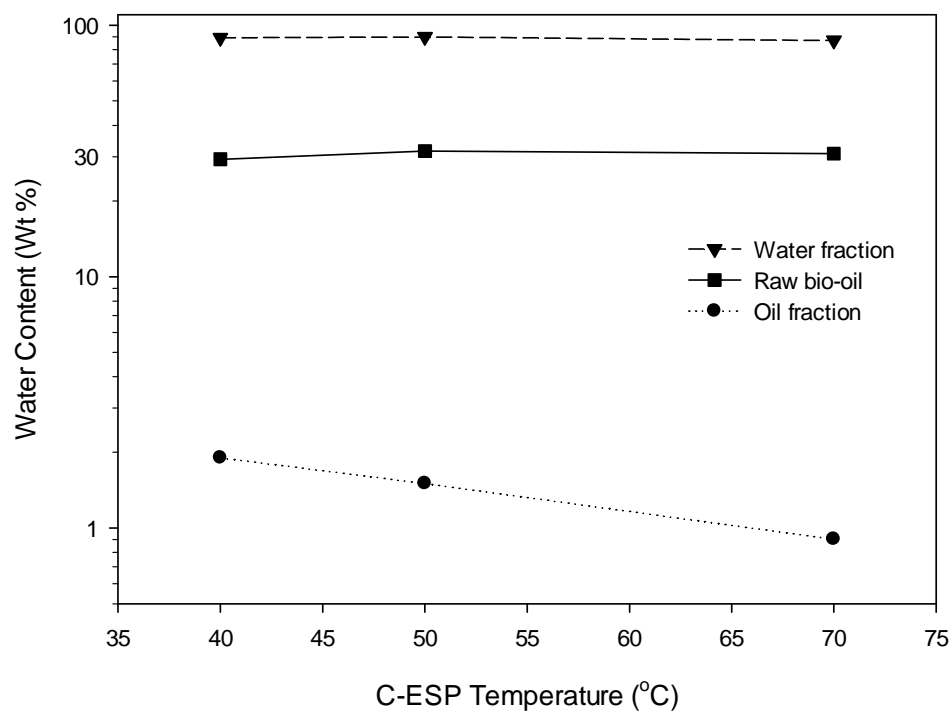


**Figure 4.7** Water content of oil fraction, water fraction, and raw bio-oil at different C-ESP temperatures

#### 4.3.1.3 Variation in heating value of bio-oil fractions

Figure 4.8 shows the higher heating values of the oil fraction, water fraction and raw bio-oil at different C-ESP operating temperatures. The heating value of the raw bio-oil is calculated using the individual heating values of the bio-oils from the three condensers. At all the C-ESP temperatures, the heating values of the oil fraction and raw bio-oil are around 30 and 20 MJ/Kg, respectively. As a result of removing water from the raw bio-oil, the heating value of the dry bio-oil increases by 50%. The heating value of the water fraction slightly increases with the increase in the C-ESP temperature, because of the increase in the loss of light organics from the C-ESP, which are then recovered in condenser 3.

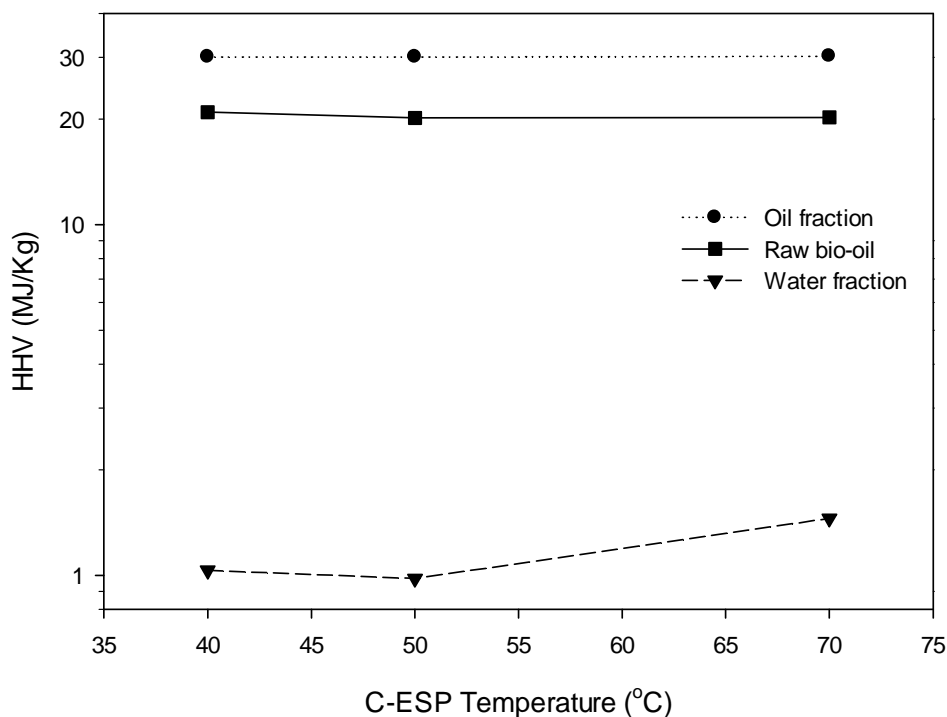
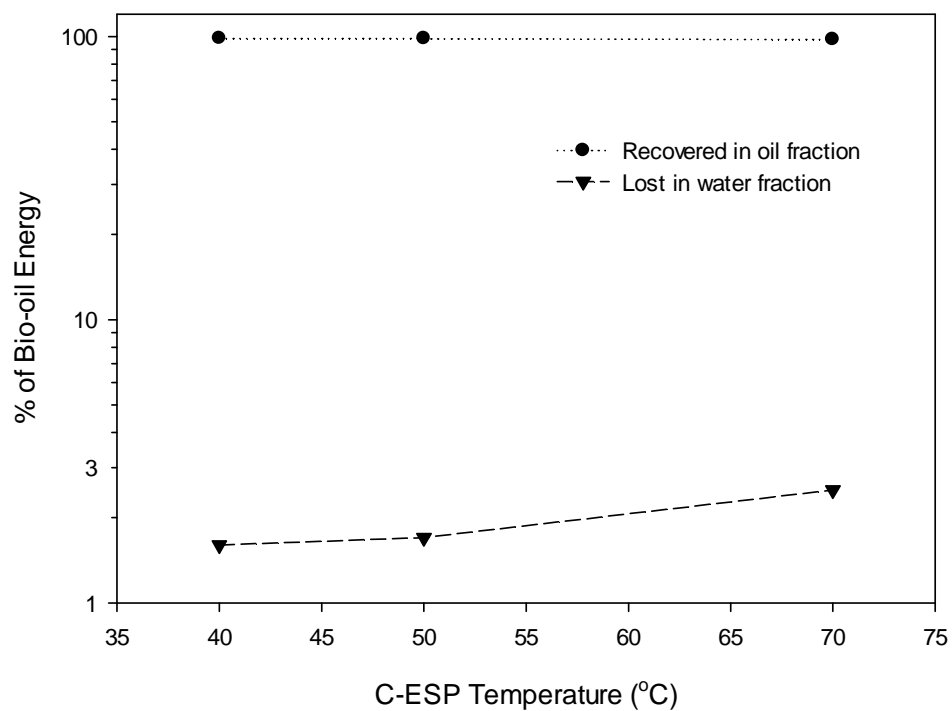


Figure 4.8 Heating value of raw bio-oil, oil and water fractions at different C-ESP temperatures

#### 4.3.1.4 Energy recovered in oil fraction

It is important to recover the maximum bio-oil energy in the dry bio-oil. Figure 4.9 shows the percentage of the raw bio-oil energy that is recovered in the oil fraction and the percentage that is lost in the water fraction, for the three different C-ESP temperatures. At the selected optimum C-ESP temperature of 70 °C, the energy recovered in the oil fraction is 98% of the total bio-oil energy. In case of fractional condensation of bio-oil vapors produced from birch bark pyrolysis, described in Chapter 3, the energy recovered in the oil fraction was 90% of the total bio-oil energy. Therefore, in terms of energy recovered in the oil fraction, lignin proves to be a better biomass feedstock when compared to the birch bark.



**Figure 4.9** Energy recovered in the oil and water fractions at different C-ESP temperatures

#### 4.3.1.5 Distribution of Phenolic compounds

GC-MS/FID analyses were carried out to identify the compounds present in the three bio-oil fractions obtained at the optimum C-ESP temperature of 70 °C. The total ion chromatograms of the bio-oil samples from the three condensers are shown in Figure 4.10. More than 99% of the compounds detected in the first condenser and C-ESP were phenolic compounds. The distribution of phenolic compounds in the oil, water fractions on the basis of raw bio-oil is shown in Figure 4.11. The oil fraction contains 94% of the phenolic compounds present in the raw bio-oil. As a result of fractional condensation of bio-oil vapors from Kraft lignin, the bio-oil fractions rich in phenolic compounds is recovered in the first condenser and C-ESP.

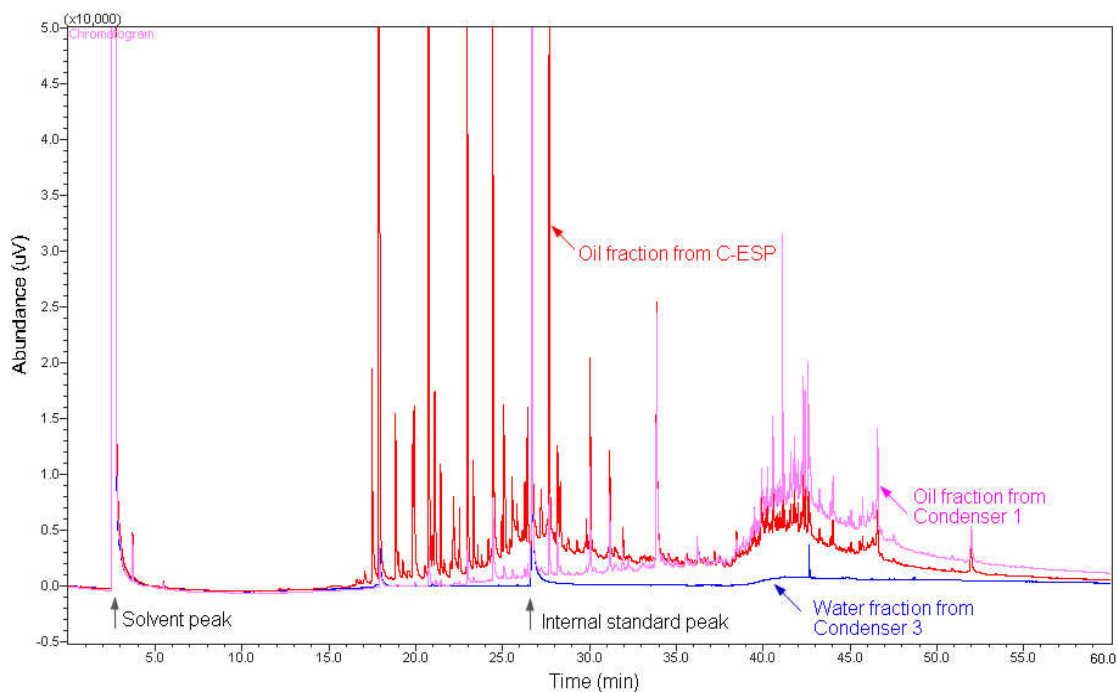


**Figure 4.10** Total ion chromatograms of bio-oil samples from the three condensers for a C-ESP temperature of 70 °C

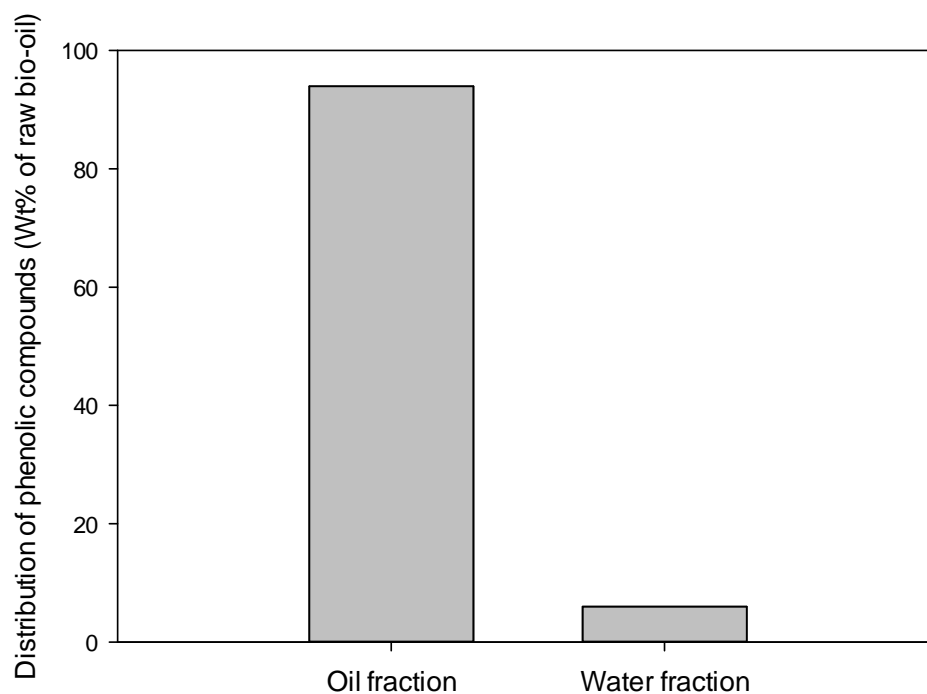


**Figure 4.11** Distribution of phenolic compounds from the pyrolytic vapors in oil and water fraction for a C-ESP temperature of 70 °C

At a C-ESP temperature of 70 °C, 94% of the phenolic compounds originally present in the bio-oil are recovered in the dry bio-oil, which has a high heating value and water content of less than 1 wt%.

#### 4.3.2 Optimization of operating conditions of pyrolysis

To investigate the effects of pyrolysis reaction temperature on the dry bio-oil yield and characteristics, experimental runs were carried out at pyrolysis temperatures of 450, 500, 550 and 600 °C. All the experiments were performed at vapor residence time of 1.5 seconds. Throughout the study, the temperatures of condenser 1, C-ESP, and condenser 3 were maintained at 80, 70, and 0 °C, respectively.

#### 4.3.2.1 Bio-oil distribution in different condensers

Figure 4.12 shows that the yields of the raw bio-oil, oil fraction and water fraction at all the pyrolysis conditions. For the oil fraction, the highest yield of 23.5% was obtained at the pyrolysis temperature of 550 °C. There is only a minimal difference in the yield of the oil fraction at pyrolysis temperatures of 500 and 550 °C. At all the reaction temperatures, the yield of the water fraction is in the range of 12% to 14%.

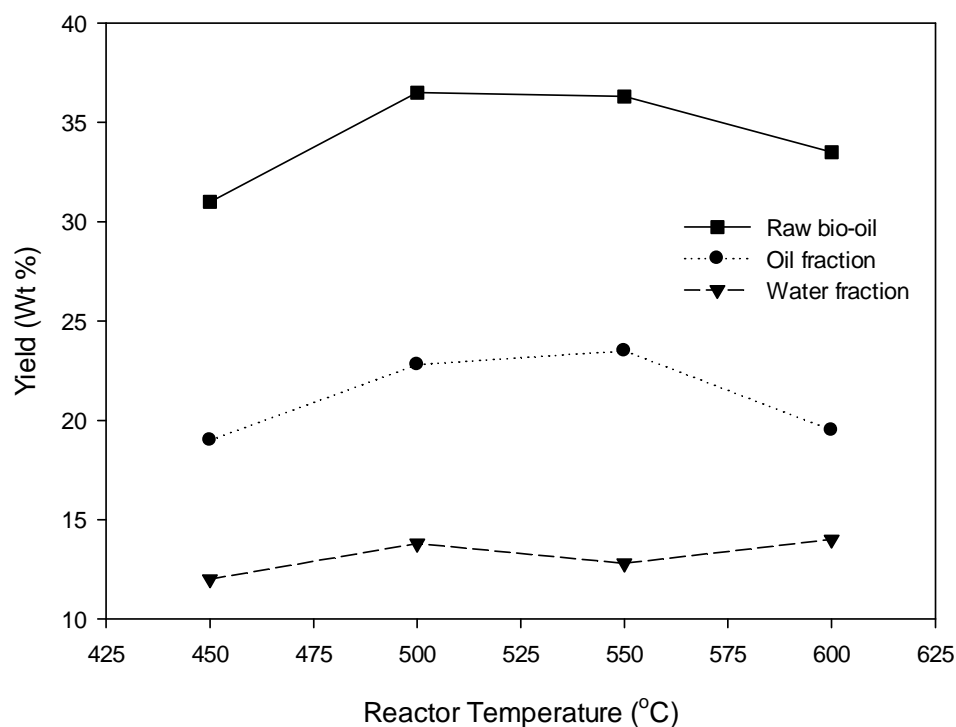


**Figure 4.12** Yields of raw bio-oil, oil and water fractions at different pyrolysis temperatures

#### 4.3.2.2 Water content of bio-oil fractions

Figure 4.13 shows that the water content of the oil fraction increases from 0.6% to 1.1% when the pyrolysis temperature is increased from 450 to 600 °C. The water content

of the raw bio-oil is around 30% at the pyrolysis temperature of 450, 500 and 550 °C, but increases to 38% at 600 °C. At all the pyrolysis temperatures, the water content of the water fraction is in between 86% and 91%.

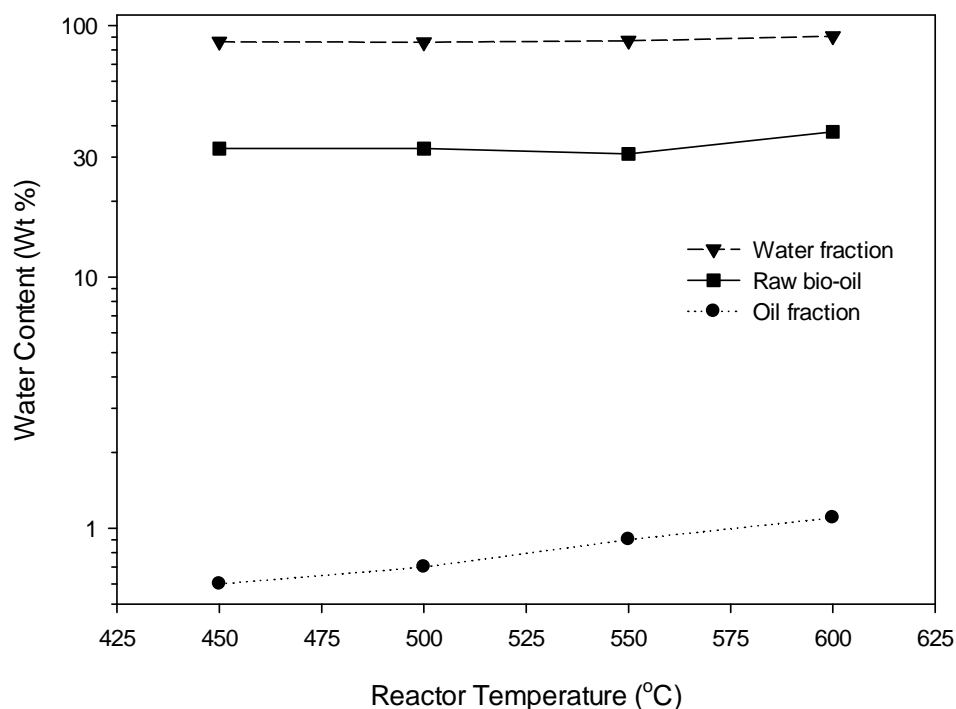


**Figure 4.13** Water content of raw bio-oil, oil and water fractions at different pyrolysis temperatures

#### 4.3.2.3 Variation in heating value of bio-oil fractions

Figure 4.14 shows that at all the pyrolysis temperatures, the heating values of the oil fraction and raw bio-oil are almost constant at around 30 and 20 MJ/Kg, respectively. Increasing the pyrolysis temperature from 450 to 600 °C, gradually decreases the heating value of the water fraction.

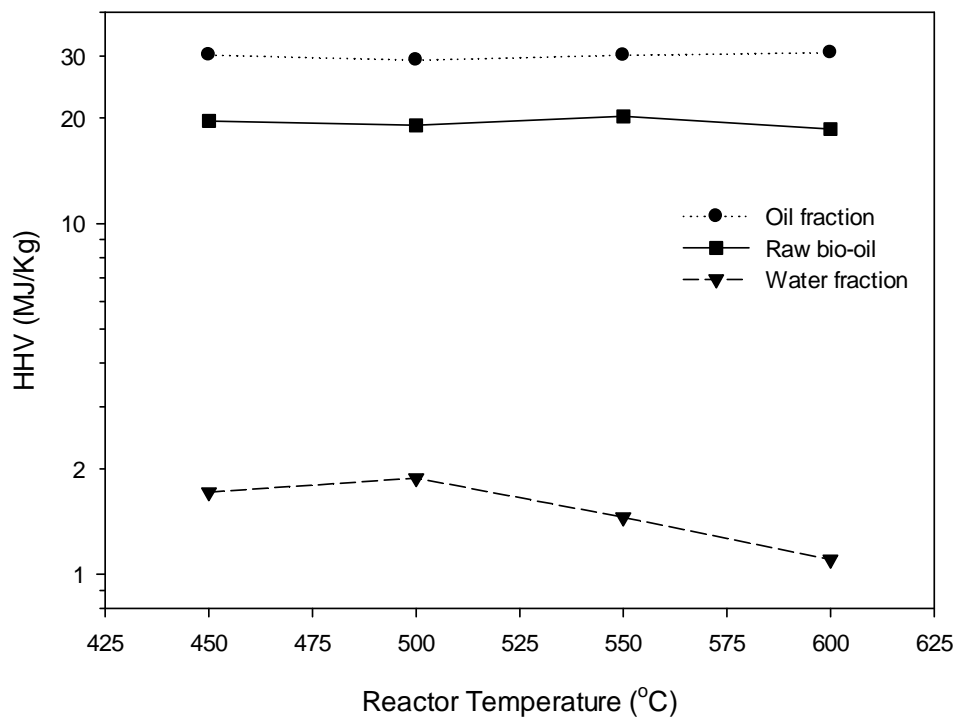


**Figure 4.14** Heating value of raw bio-oil, oil and water fractions at different pyrolysis temperatures

#### 4.3.2.4 Energy recovered in oil fraction

As mentioned in the earlier section, most of the energy originally present in the raw bio-oil is recovered in the oil fraction. Figure 4.15 shows that 96% to 98% of the raw bio-oil energy is recovered in the oil fraction at all the pyrolysis conditions.

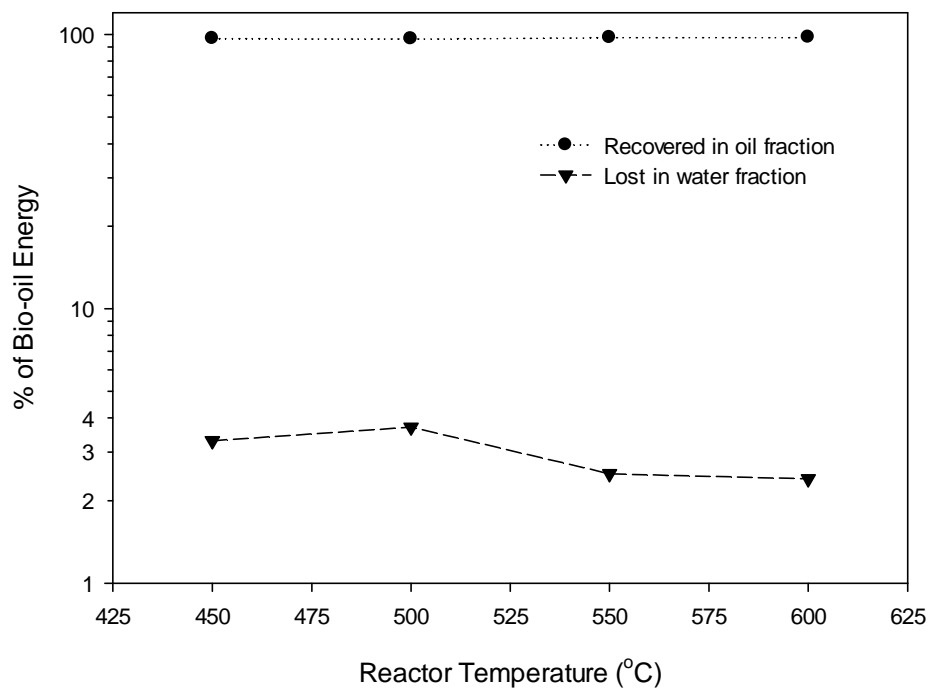


**Figure 4.15** Energy recovered in oil fraction at different pyrolysis temperatures

The maximum yield of the dry bio-oil is obtained at the pyrolysis temperature of 550 °C. With the change in the pyrolysis temperature from 450 to 600 °C, there is no considerable change in the energy recovered in the dry bio-oil, its water content or its heating value.

#### 4.3.3 Fractioned lignin bio-oil as a biofuel

Figure 4.16 compares the heating values of the dry bio-oil with other commercial fuels. The heating value of ethanol is around 30 MJ/Kg, which is same as the heating value of the dry bio-oil obtained from the pyrolysis of Kraft lignin. Currently, ethanol is being used as biofuel additive for gasoline.

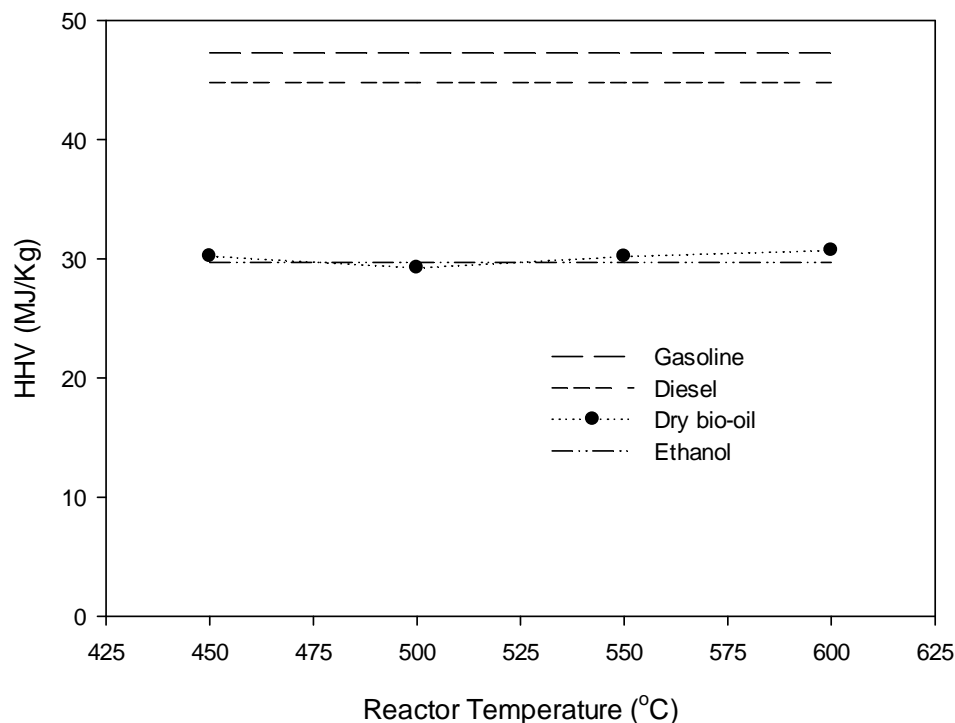


**Figure 4.16** Heating value of dry bio-oil and other commercial fuels

#### 4.4 Conclusions

Kraft lignin was pyrolyzed in a bubbling bed reactor coupled with an internal stirrer and the resulting bio-oil vapors were fractionated with a series of three temperature-controlled condensers. The condenser train consisted of an electrostatic precipitator-cum-condenser (C-ESP) between two cyclonic condensers. The temperatures of the condensers were optimized to obtain a nearly water free (less than 1 wt%) dry bio-oil in the first two condensers and a water-rich product in the third condenser. The dry bio-oil was found to contain 94% of the phenolic compounds present in the raw bio-oil.

The maximum yield of dry bio-oil was obtained at the pyrolysis reactor temperature of 550 °C. The energy recovered in the dry bio-oil was around 98% of the energy

originally present in the raw bio-oil. As the dry bio-oil fraction is rich in phenolic compounds and has the same heating value as ethanol makes fast pyrolysis combined with fractional condensation a promising process to produce high quality fuels and chemicals.

#### **4.5 Acknowledgments**

The authors would like to acknowledge funding from the Lignoworks network ([www.lignoworks.ca](http://www.lignoworks.ca)). They would also like to acknowledge help from Rob Taylor, and Caitlin Marshall.

#### **4.6 References**

- (1) Amen-Chen C, Pakdel H, Roy C. Production of monomeric phenols by thermochemical conversion of biomass: A review. *Bioresour Technol* 2001;79(3):277-299.
- (2) Lora JH, Glasser WG. Recent industrial applications of lignin: A sustainable alternative to nonrenewable materials. *Journal of Polymers and the Environment* 2002;10(1-2):39-48.
- (3) Bridgwater AV. Review of fast pyrolysis of biomass and product upgrading. *Biomass Bioenergy* 2012;38:68-94.
- (4) Nowakowski DJ, Bridgwater AV, Elliott DC, Meier D, de Wild P. Lignin fast pyrolysis: Results from an international collaboration. *J Anal Appl Pyrolysis* 2010;88(1):53-72.
- (5) Palmisano P, Berruti FM, Lago V, Berruti F, Briens C. Lignin Pyrolysis in a Fluidized Bed Reactor. *Tcbiomass*; 2011.

- (6) Bridgwater AV. Renewable fuels and chemicals by thermal processing of biomass. *Chem Eng J* 2003 3/15;91(2–3):87-102.
- (7) Oasmaa A, Czernik S. Fuel oil quality of biomass pyrolysis oils - state of the art for the end users. *Energy and Fuels* 1999;13(4):914-921.
- (8) Chen T, Deng C, Liu R. Effect of selective condensation on the characterization of bio-oil from pine sawdust fast pyrolysis using a fluidized-bed reactor. *Energy and Fuels* 2010;24(12):6616-6623.
- (9) Jendoubi N, Broust F, Commandre JM, Mauviel G, Sardin M, Lédé J. Inorganics distribution in bio oils and char produced by biomass fast pyrolysis: The key role of aerosols. *J Anal Appl Pyrolysis* 2011;92(1):59-67.
- (10) Westerhof RJM, Brilman DWF, Garcia-Perez M, Wang Z, Oudenhoven SRG, Van Swaaij WPM, et al. Fractional condensation of biomass pyrolysis vapors. *Energy and Fuels* 2011;25(4):1817-1829.
- (11) Pollard AS, Rover MR, Brown RC. Characterization of bio-oil recovered as stage fractions with unique chemical and physical properties. *J Anal Appl Pyrolysis* 2012;93:129-138.
- (12) Berruti FM, Ferrante L, Berruti F, Briens C. Optimization of an intermittent slug injection system for sawdust biomass pyrolysis. *International Journal of Chemical Reactor Engineering* 2009;7.
- (13) Xu R, Ferrante L, Briens C, Berruti F. Flash pyrolysis of grape residues into biofuel in a bubbling fluid bed. *J Anal Appl Pyrolysis* 2009;86(1):58-65.
- (14) Bedmutha RJ, Ferrante L, Briens C, Berruti F, Inculet I. Single and two-stage electrostatic demisters for biomass pyrolysis application. *Chemical Engineering and Processing: Process Intensification* 2009;48(6):1112-1120.
- (15) Bridgwater AV, Meier D, Radlein D. An overview of fast pyrolysis of biomass. *Org Geochem* 1999 26 November 1998 through 27 November 1998;30(12):1479-1493.

## **5 Chapter 5: Conclusions**

A fractional condensation train for bio-oil vapors was developed to achieve the separation of some of the key components of the bio-oil and, consequently, improve the properties and the value of each of the separated product streams.

The separation of a mixture of three model compounds of bio-oil from a vapor and carrier gas stream was investigated with the help of a series of three condensers maintained at different temperatures. The practical performance of the fractional condensation train was improved by comparing the experimental results with the theoretical results predicted by the HYSYS modeling tool. It showed that good heat transfer and mixing was essential, and could be achieved by using condensers with a cyclonic entry. It also showed that a good demister was essential to achieve effective separation.

The fractional condensation of bio-oil vapors produced from the pyrolysis of birch bark was investigated, using a special condenser - electrostatic demister in the condensing train. The bio-oil recovered in the first and second condensers was found to contain less than 1 wt% water. The fact that this dry bio-oil fraction has a heating value slightly better than the ethanol makes fractional condensation a promising process to produce high quality fuels.

The pyrolysis of Kraft lignin combined with the fractional condensation of its bio-oil vapors was investigated. The bio-oil recovered in the first and second condensers contained 94% of the phenolic compounds present in the original bio-oil. The heating value of the phenolic rich bio-oil rich was almost same as the heating value of ethanol,

which is currently used as bio-fuel additive for gasoline. The process of fractional condensation proved to be successful in separating oil fraction rich in phenols, which has a high commercial value.

### **5.1 Recommendations for future work**

- Perform detailed analysis of fractionated bio-oil samples to determine the distribution of various chemicals in the three condensers.
- Perform stability tests to determine the effect of removing water on the stability of fractionated bio-oil samples.
- Perform the fractional condensation of bio-oil vapors produced from different kinds of biomass and optimize the condenser train to recover single compound rich bio-oil fractions.
- Perform gasification of watery bio-oil fraction to recover the lost energy.

## Curriculum Vitae

**Name:** Akhil Tumbalam Gooty

**Post-secondary Education and Degrees:** The University of Western Ontario  
London, Ontario, Canada  
2010-2012 M.E.Sc

Anna University  
Chennai, Tamil Nadu, India  
2002-2006 B.Tech

**Honours and Awards:** Western Graduate Research Scholarship (WGRS)  
2010-2012

**Related Work Experience** Graduate Research Assistant  
The University of Western Ontario  
2010-2012

Graduate Teaching Assistant  
The University of Western Ontario  
2011